

Accepted Manuscript

Syntheses, crystal structures and photo physical aspects of azido-bridged tetranuclear cadmium (II) complexes: DFT/TD-DFT, thermal, antibacterial and *anti*-biofilm properties

Dhrubajyoti Majumdar, Swapan Dey, S.S. Sreejith, Jayanta Kumar Biswas, Monojit Mondal, Pooja Shukla, Sourav Das, Tapan Pal, Dhiraj Das, Kalipada Bankura, Dipankar Mishra

PII: S0022-2860(18)31314-0

DOI: <https://doi.org/10.1016/j.molstruc.2018.11.010>

Reference: MOLSTR 25839

To appear in: *Journal of Molecular Structure*

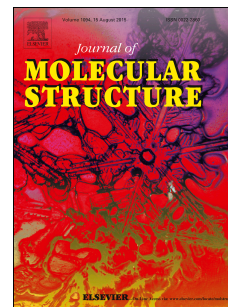
Received Date: 5 August 2018

Revised Date: 2 November 2018

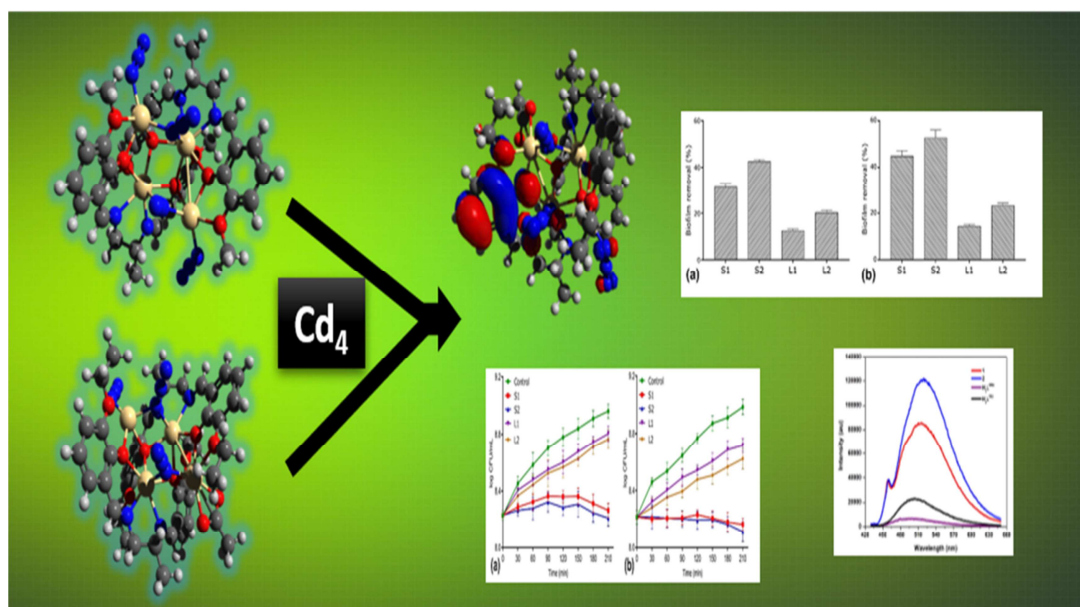
Accepted Date: 5 November 2018

Please cite this article as: D. Majumdar, S. Dey, S.S. Sreejith, J.K. Biswas, M. Mondal, P. Shukla, S. Das, T. Pal, D. Das, K. Bankura, D. Mishra, Syntheses, crystal structures and photo physical aspects of azido-bridged tetranuclear cadmium (II) complexes: DFT/TD-DFT, thermal, antibacterial and *anti*-biofilm properties, *Journal of Molecular Structure* (2018), doi: <https://doi.org/10.1016/j.molstruc.2018.11.010>.

This is a PDF file of an unedited manuscript that has been accepted for publication. As a service to our customers we are providing this early version of the manuscript. The manuscript will undergo copyediting, typesetting, and review of the resulting proof before it is published in its final form. Please note that during the production process errors may be discovered which could affect the content, and all legal disclaimers that apply to the journal pertain.



GRAPHICAL ABSTRACT



Syntheses, crystal structures and photo physical aspects of azido-bridged tetranuclear cadmium (II) complexes: DFT/TD-DFT, thermal, antibacterial and anti-biofilm properties

Dhrubajyoti Majumdar ^{a,b}, Swapan Dey ^{b,*}, S. S. Sreejith ^c, Jayanta Kumar Biswas ^d, Monojit Mondal ^d, Pooja Shukla ^e, Sourav Das^{e,*}, Tapan Pal ^f, Dhiraj Das ^g, Kalipada Bankura ^a, Dipankar Mishra ^{a,*}

^{a,b}Department of Chemistry, Tamralipta Mahavidyalaya, Tamluk-721636, West Bengal, India

^bDepartment of Applied Chemistry, Indian Institute of Technology (Indian School of Mines), Dhanbad, Jharkhand 826004, India

^cDepartment of Applied Chemistry, Cochin University of Science and Technology, Kochi, 682022, Kerala, India

^dDepartment of Ecological Studies & International Centre for Ecological Engineering, University of Kalyani, Kalyani 741235, West Bengal, India

^eDepartment of Chemistry; Institute of Infrastructure Technology Research and Management; Near Khokhara Circle, Maninagar East, Ahmedabad-380026, Gujarat, India

^fDepartment of Chemistry, BIT Sindri, Dhanbad-828123, Jharkhand, India

^g Department of Chemical Sciences, IISER, Mohali, Manauli, PO 140306, India

AUTHOR EMAIL ADDRESS: dmishra.ic@gmail.com, deyswapan77@yahoo.com,
d.sourav245@gmail.com

ABSTRACT

In this work we have reported two novel tetranuclear Cd(II) complexes viz. $[\text{Cd}_4(\text{L}^{\text{OMe}})_2(\mu_{1,1}\text{-N}_3)_3(\mu_{1,3}\text{-N}_3)]_n$ (**1**) and $[\text{Cd}_4(\text{L}^{\text{OEt}})_2(\mu_{1,1}\text{-N}_3)_3(\text{OAc})_2]$ (**2**) where $(\text{H}_2\text{L}^{\text{OMe}})$ and $(\text{H}_2\text{L}^{\text{OEt}})$ are two important less explored salen-type Schiff base ligands. Both of the complexes have been characterized by using common spectroscopic techniques, elemental analyses (C, H and N), X-ray powder diffraction pattern (PXRD) and thermal analysis by TGA along with single x-ray crystallography. The complete structural study discloses that in both cases the fully deprotonated ligand $[\text{L}^{\text{OMe}}]^{2-}$ or $[\text{L}^{\text{OEt}}]^{2-}$ utilized all potential coordination sites to accommodate four Cd(II) ions. Complex **1** is a one-dimensional polymer with azide (N_3) linkage having both $(\mu_{1,1}$ end on) and $(\mu_{1,3}$ end-to-end) azido bridging but complex **2** is a discrete octanuclear ensemble where two $[\text{Cd}_4(\text{O})_4(\text{N})_2]^{2+}$ units bridged to each other showing $\mu_{1,1}$ end on end on azide bridging. Exploration of photo physical properties in DMSO solvent reveals that Cd(II) complexes enhance appreciably the fluorescence behavior over free Schiff base ligands $(\text{H}_2\text{L}^{\text{OMe}})$ and $(\text{H}_2\text{L}^{\text{OEt}})$. DFT calculations performed at B3LYP/def2-TZVP level of theory reveal both the energetics and composition of FMOs in these complexes and also show electrophilic and nucleophilic areas *via* molecular electrostatic maps [ESP]. The antibacterial, membrane damage assay and anti-biofilm properties of complexes **1** and **2** were investigated very carefully against some important Gram-positive and Gram-negative bacterial strains.

Keywords: Antimicrobial, azide, Cd(II) coordination compounds, DFT, photoluminescence, TGA

1. Introduction

In the past few decades, the design and construction of polymeric and discrete metal-organic frameworks (MOFs) of d^{10} group 12 metal ions like zinc, cadmium or Hg are of great interest and booming field of investigation due to the prosthetic beauty and potential applications as functional materials [1-3]. Thus, a major focused have drawn towards N,O-donor salen-type Schiff base complexes due to their preoperational accessibilities, structural varieties, extreme stability, plasticity, varied denticities [4a] and have broad spectrum of bioactivities such as antibacterial, antimicrobial, anti-allergic, antiviral, anti-oxidative, anticonvulsant, antitumor and anticancer[4b-d]. There are some novel researches which potentially supported that microbicidal and anticancerous activities of Schiff base ligands are appreciably enhanced after complex formation with transition metal ions. Thus synthetic chemists will have a target to discover always new complexes that have medicinal effects or less toxic. In nature biofilms are the most important common path of bacterial growth which is responsible to various clinical infections [4e]. Due to this adverse effect scientists have found Cd(II) Schiff base complexes antibiofilm properties promoted significantly by different types of bacteria. This antibiofilm activity effectively explored by salen-type (N_2O_2) Schiff bases and their associated complexes which is potentially significant in biomedical field [4f]. Thus scientists around the world are tried to find out new antibiotics related to new Schiff-base complexes which have significant antimicrobial potency. On the other hand utilizing salen-type (N_2O_2) Schiff base ligands, inorganic synthetic chemists have devised zero to three-dimensional coordination polymers (CPs) in presence of multifunctional organic or inorganic linkers as auxiliary moieties [5]. In this context, azide is widely used as a worthy coordinating ancillary co-ligand due to their smaller length, rigidity and versatile coordination modes of donor atoms [6-30]. So, group 12 metal ion such as Cd(II)

polymeric or discrete complexes which are derived from azide ancillary co-ligands are of current interest because of their unique pale color, higher thermal stability and possible strong luminescence properties [31-42]. Till date several azido bridged discrete and coordination polymers (CPs) have been reported but exploration of Cd(II)-azido bridged complexes are always deserves attention due to the uncertainty of the product formation and versatility of getting new different dimensional structural products and their associated novel photo physical, antimicrobial and anti-biofilm properties which are of profound interest to both structural and synthetic chemists.

In our previous publications, our highly motivated research group have successfully explored the luminescent and antimicrobial, antibiofilm properties of halides and pseudohalides metal complexes of $3d^{10}$ metal ions where use of Schiff base ligand [N, N'-Bis(3-methoxysalicylidenimino)-1,3-diaminopropane] (H_2L^{OMe}) allowed us to isolate a homometallic trinuclear linear complex $[Cd_3(L^{OMe})_2(Cl)_2]$ in presence of NaCl as Cl^- spacer [43]. Utilizing the identical ligand in presence of thiocyanate anion, an 1D chain of Zn(II) coordination polymer $[Zn_2L^{OMe}(\mu_{1,3}-SCN)(\eta^1SCN)]_n$ has been reported [44]. Apart from these usual works, further analyzed two Cd(II) Azide/thiocyanate linked 1D and 2D coordination polymers $\{[Cd_4(N_3)_4(L^{OMe})_2].H_2O\}_n$, $[Cd_4(L^{OMe})_2(SCN)_4]_n$, three Zn(II) dinuclear complexes $[Zn_2(L^{OEt})(CH_3OH)_2(SCN)(OAc)]$, $[Zn_2(L^{OEt})(CH_3OH)_2(N_3)_2]$, $[Zn_2(L^{OEt})(Cl)_2(CH_3OH)].CH_3OH$, Cd(II) polynuclear-discrete complexes viz, $[Cd_2L^{OEt}(\mu_{1,3}-SCN)(\eta^1-SCN)]_n$, $\{Cd_4(L^{OEt})_2(\mu_{1,1}-N_3)_3(\eta^1-N_3)_2\}_2$, $[Cd_2(L^{OEt})(Cl)_2.CH_3OH].CH_3OH$ and their novel luminescent and antimicrobial properties vividly [45-47]. Taking cues from such novel research works, we were prompted to explore the reactions of nonessential toxic Cd(II) metal ion in presence of two less explored salen-type (N_2O_2) ligands (H_2L^{OMe})/(H_2L^{OEt}) using 1,2-

diamnopropane (*Pn*) instead of 1,3-propane diamine in assisting the formation of complexes $[\text{Cd}_4(\text{L}^{\text{OMe}})_2(\mu_{1,1}\text{-N}_3)_3(\mu_{1,3}\text{-N}_3)]_n$ (**1**) and $[\text{Cd}_4(\text{L}^{\text{OEt}})_2(\mu_{1,1}\text{-N}_3)_3(\text{OAc})_2]$ (**2**).

The present article primarily focuses on the syntheses of complex **1** and **2**, X-ray crystal structure, DFT/TD-DFT calculations, photo physical, thermal behavior, antibacterial efficacy, membrane damage assay and anti-biofilm properties.

2. Experimental

2.1. General remarks and physical measurements

2.1.1. Materials

All chemicals were of reagent grade, purchased from commercial sources and used as received without further purification. High purity 3-methoxysalicylaldehyde, 3-ethoxysalicylaldehyde and 1,2-diaminopropane (*Pn*) was purchased Sigma Aldrich Company, USA. $\text{Cd}(\text{OAc})_2 \cdot 2\text{H}_2\text{O}$ was directly purchased from E. Merck, India. High purity NaN_3 was purchased from SDFCL, India. Solvent methanol was used of AR grade.

2.1.2. Instrumentation

Elemental analyses (C, H, and N) of salen-type Schiff base ligands $(\text{H}_2\text{L}^{\text{OMe}})/(\text{H}_2\text{L}^{\text{OEt}})$ and cadmium(II) complexes were determined with a Perkin–Elmer CHN analyzer 2400. FT-IR spectra of Cd(II) complexes were recorded as KBr pellets within the range $4000\text{--}400\text{ cm}^{-1}$ having 16 scans at a wave number resolution of 4 cm^{-1} on a Perkin–Elmer spectrum RX 1 using detector DTGS (Deuterated triglycine sulfate). The abbreviations commonly used in this manuscript stands for vs=very strong, s=strong, m=medium, w=weak. The electronic UV-Vis spectra of both Cd(II) complexes and free salen-type ligands $(\text{H}_2\text{L}^{\text{OMe}})/(\text{H}_2\text{L}^{\text{OEt}})$ in DMSO solvent were recorded on a Hitachi model U-3501 spectrophotometer. Perkin-Elmer LS50B spectrofluorimeter model was used directly for the fluorescence measurements of complex **1** and

2 as well as free salen-type ligands at room temperature (298K). Thermo-gravimetric analyses (TGA) of both Cd(II) complexes were carried out on a TGA-50H analyzer from ambient temperature to 700 °C at a temperature rate of 10 °C/min in a flowing 30ml/min under nitrogen atmosphere using a platinum cell. X-ray powder diffraction measurements for tetranuclear Cd(II) complexes were carried out using BRUKER AXS, GERMANY X-ray diffractometer model after scanning 2 theta from 4° to 50°. The radiation used for PXRD measurement purpose is Cu K-alpha-1. The fluorescence quantum yields (Φ) of Cd(II) complexes have been determined using the following well known mathematical equation (1) associated with fluorescence spectroscopy where Quinine sulfate is used as the secondary standard ($\Phi = 0.57$ in water) [48] .

$$\frac{\Phi_S}{\Phi_R} = \frac{A_S}{A_R} \times \frac{(Abs)_R}{(Abs)_S} \times \frac{n_S^2}{n_R^2} \quad (1)$$

According to equation (1) abbreviations used stands for: A terms denote the fluorescence area under the curve; Abs denotes absorbance; n is the refractive index of the medium; Φ is the fluorescence quantum yield; and subscripts S and R denote parameters for the studied sample and reference, respectively.

2.2. X-ray crystallography

The crystal data of azido-bridged tetranuclear Cd(II) complexes (**1-2**) have been collected on a Bruker *SMART* CCD [49] diffractometer (Mo K α radiation, $\lambda = 0.71073$ Å). The program *SMART* was used for collecting frames of data, indexing reflections, and determining lattice parameters, *SAINT* [50] for integration of the intensity of reflections and scaling, *SADAB*[51] for absorption correction, and *SHELXTL* for space group and structure determination and least-squares refinements on F^2 . The crystal structures of cadmium (II) complexes (**1-2**) were fully

solved and refined by full-matrix least-squares methods against F^2 by using the program *SHELXL-2014*[52] and *Olex-2* software [53]. All the non-hydrogen atoms were refined with anisotropic displacement parameters. Hydrogen positions were fixed at calculated positions and refined isotropically. Different types of crystallographic figures for cadmium(II) complexes (**1-2**) were generated using latest Diamond software[54]. A summary of the crystallographic data and complete structural refinement parameters of cadmium(II) complexes (**1-2**) are clearly presented in Table S1[see supplementary material]. Crystallographic data (excluding structure factors) of tetranuclear cadmium (II) complexes (**1-2**) have been deposited with the Cambridge Crystallographic Data Centre as supplementary publication nos. CCDC 1811084-1811085. Copies of the data can be obtained, free of charge, on application to CCDC, 12 Union Road, Cambridge CB2 1EZ, U.K.: <http://www.ccdc.cam.ac.uk/cgi-bin/catreq.cgi>, e-mail: data_request@ccdc.cam.ac.uk, or fax: +44 1223 336033.

2.2.1. Computational DFT methods

Frontier orbital analyses and global reactivity indices of both tetranuclear Cd(II) complexes were explored using DFT calculations employing ORCA 3.0.3 software package [55] using the Becke's three-parameter hybrid exchange functional including the Lee–Yang–Parr nonlocal correlation functional (B3LYP) [56] and the triple zeta valence basis set with one set of polarization function (TZVP) [57]. To accelerate the calculations, we utilized the resolution of identity (RI) approximation with the decontracted auxiliary def2–TZV/J Coulomb fitting basis sets and the chain–of–spheres (RIJCOSX) approximation to exact exchange as implemented in ORCA [57]. The Initial geometries of the complexes were taken from their crystal coordinates and the optimized geometries were confirmed to be global energy minima by performing the frequency calculations which had no imaginary frequency. The choice of the TZVP basis set was

made since it reduces the basis set superposition error (BSSE) to negligible in the calculation of systems with noncovalent interactions. The visualization of orbitals was done using Avogadro software [58]. For calculating the composition of Frontier orbitals and distribution of ESP (Electrostatic potential), Multiwfn program [59, 60] was used and .molden type file generated using orca_2mkl functionality was employed as the input for the program. The Time Dependent-Density Functional Theory (TD-DFT) calculation of both tetranuclear Cd(II) complexes were performed using Gaussian 09 [60(b)] at DFT/B3LYP level using 6-31+G* basis set for C, H, O and N atoms and SDD basis set and an effective core potential was used for Cd atom. The effect of the solvent was modeled with the polarized continuum model (PCM) [60(b)]. The crystallographic coordinates have been considered for the TD-DFT calculation. All generated molecular orbitals (MOs) during TD-DFT calculations were visualized using common software Gauss view 5.0.

2.2.2. Experimental of antibacterial and anti-biofilm properties of tetranuclear Cd(II) complexes

Two Gram positive bacterial strains (*Bacillus subtilis* MTCC 441 and *Enterococcus gallinarum* MTCC 7049) and two Gram negative bacterial strain (*Enterobacter aerogenes* MTCC 111 and *Proteus vulgaris* MTCC 744) was selected for *in vitro* evaluation of antibacterial potentials of two complexes **1** and **2** and two of their respective ligands (H_2L^{OMe}/H_2L^{OEt}). The bacterial strains were obtained from Microbial Type Culture Collection and Gene Bank (MTCC), Institute of Microbial Technology, Chandigarh, India. For the antimicrobial assay, two Cd(II) complexes as well as the corresponding ligands (H_2L^{OMe}/H_2L^{OEt}) were dissolved in dimethyl sulfoxide (DMSO) solvent. Selected concentrations of complexes (**1-2**) were prepared in sterilized Luria-Bertani medium (modified). The bacterial culture ($\sim 5 \times 10^5$ colony forming units, CFU)/mL) was inoculated to the respective medium maintaining the final concentration of DMSO set within 1%.

All the bacterial strains were cultured in an incubator at 37°C and under mechanical shaking (150 rpm) for 24 h. Antibacterial potential and minimum inhibitory concentrations (MIC) of the complexes (**1-2**) and the Schiff base ligands (H_2L^{OMe}/H_2L^{OEt}) were probed against the selected bacterial strains belonging to different categories following standard protocol prescribed by Clinical and Laboratory Standards Institute (CLSI) (CLSI, 2012) [61]. The MICs were determined measuring the turbidity in the broth using UV-Vis spectrophotometer at 600nm. The threshold concentrations of the respective Cd(II) complexes (**1-2**) and their Schiff base ligands (H_2L^{OMe}/H_2L^{OEt}) at which the bacterial growth ($OD_{600} < 0.05$) was inhibited under 24 h incubation were considered as individual MICs [62]. Individual susceptibilities of the bacterial strains to the complexes(**1-2**) and their ligands (H_2L^{OMe}/H_2L^{OEt}) were tested following agar well diffusion method and the antibacterial efficiencies of those chemical entities were defined by measuring the diameter (mm) of the growth inhibition zone developed in the process [63].

The time-kill curves of the bacterial strains were obtained based on the growth pattern following chemical treatment of the bacterial strains remaining in their mid log phase with the said complexes (**1-2**) and ligands (H_2L^{OMe}/H_2L^{OEt}) at their respective MICs [62]. The bacterial cultures without any chemical treatment served as control. Optical density of the cultures was determined with a 30 min interval frequency using UV-Vis spectrophotometer at 600nm. The viable cell numbers were enumerated adopting the spread plate method and counting the bacterial colony forming units (CFU/mL) developed on the agar plate.

Biofilm biomass was determined following the standard method [64]. The bacterial cells of each representative belonging to Gram positive (*E. gallinarum*) and Gram negative (*P. vulgaris*) were cultured for 16 h in brain-heart infusion medium. The inoculums of the bacterial cultures (1 mL) were added to the fresh media (100 mL) and incubated at 37 °C. The bacterial cell suspension (2

mL; $OD_{600} = 0.1$) derived from the prepared culture passing through the mid-log phase was then transferred to a sterile Petri plates (35 mm) and kept under incubation at 37 °C to allow biofilm formation. The used media was disposed of the plates and media containing respective concentrations (MIC) of the Cd(II) complexes (**1-2**) and ligands (H_2L^{OMe}/H_2L^{OEt}) were added afresh to the plates, maintaining triplicates for each treatment. A positive control was set with biofilm without any chemical treatment, and a negative control was maintained only with sterile broth. The plate was subsequently incubated at 37 °C for 24 h under static condition. Thereafter aspiration was done for the contents of each plate. The plates were subjected to vigorous shaking with 2 mL of phosphate buffer saline (PBS) to ward of all the non-adhering bacteria. Fixation of the biofilm containing attached bacteria was performed with methanol (2 mL) for 15 min. It was followed by staining of the biofilm with 2 mL of 2% crystal violet for 5 min at room temperature. Differentiation of the biofilm matrices adhered to the plate surface was accomplished by slowly ringing the plate in sterile Mili-Q water. Drying of the plates was done leaving them in the open air at room temperature. Resolubilization of the dye adhering the biofilm was performed with 2 mL of 33% (v/v) glacial acetic acid and absorbance was measured at 570 nm using UV-Vis spectrophotometer.

Both bacterial strains *E. gallinarum* and *P. vulgaris* were grown overnight in a sterile plate (35 mm) to develop biofilm [65]. The selected complexes (**1-2**) and corresponding ligands (H_2L^{OMe}/H_2L^{OEt}) were added following the method as described in connection with antibiofilm assay. Positive and negative control sets were maintained as defined before. The spent media was dispensed from the plates and washed with PBS to remove planktonic bacteria. The plates were dried in the air. Fresh media (2 mL) containing tetrazolium dye 3-(4,5-dimethylthiazol-2-yl)-2,5-diphenyltetrazolium bromide (MTT; 0.5 mg/mL) was added to each plate and incubated in the

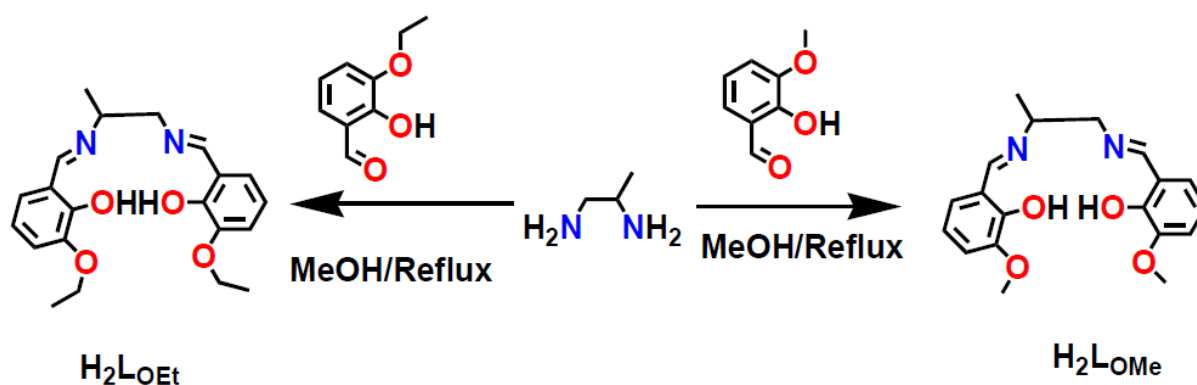
dark for 2 h at 37 °C. The MTT solution was discarded and DMSO (2 mL) was added immediately to the plate to solubilize the formazan crystals developed in the plate and mixed thoroughly. It was left for incubation for 15 min at 25 °C [66]. The absorbance of the solution was measured using a UV-Vis spectrophotometer at 570 nm.

Membrane damage assay was performed to test the efficiency of the Cd(II) complexes (**1-2**) and their Schiff base ligands in inflicting damage to bacterial cell membrane integrity. Membrane damage was evaluated by quantification of nucleic acids released from the cell.^[62] This assay was performed on one representative each from Gram positive (*E. gallinarum*) and Gram negative (*P. vulgaris*) bacterial category [67]. Overnight cultures of the both bacterial strains were subjected to centrifugation at 8000 rpm for 5 min. The cell pellet was washed three times by phosphate buffer saline (PBS, pH 7.4) and resuspended in the liquid media. The bacterial suspension with a defined optical density (0.7 at 600 nm) was distributed into different conical flasks. The concentrations of the complexes (1-2) and ligands were set at their respective MICs against the bacterial strains. Control set was maintained without any chemical treatment. Samples (2 mL) were collected at 30 min interval and filtered using syringe filter (0.2 µm), and the filtrate was measured using UV-Vis spectrophotometer at 260 nm to estimate the nucleic acids released out.

2.3. Synthetic Methodologies

2.3.1. Syntheses of salen-type Schiff base ligands (H_2L^{OMe}/H_2L^{OEt})

The Schiff base ligands (H_2L^{OMe} and H_2L^{OEt}) was synthesized by the condensation of 1 mmol (0.152g) 3-methoxysalicylaldehyde or (0.1662g) 3-ethoxysalicylaldehyde with 0.5 mmol (0.0371g) 1,2-propanediamine (*Pn*) in (50 mL) of methanol for ca. 1 h (see Scheme 1). The dark yellow colored solution was then used directly for tetranuclear azido-bridged Cd(II) complex formation.



Scheme 1. Synthetic representation of salen-type ligands ($\text{H}_2\text{L}^{\text{OMe}}/\text{H}_2\text{L}^{\text{OEt}}$)

2.3.2. Synthesis of complex $[\text{Cd}_4(\text{L}^{\text{OMe}})_2(\mu_{1,1}\text{-N}_3)_3(\mu_{1,3}\text{-N}_3)]_n$ (**1**)

To the methanolic solution (30 mL) of cadmium acetate dihydrate (0.266g, 1 mmol), dark orange yellow solution of Schiff base ($\text{H}_2\text{L}^{\text{OMe}}$) was added directly followed by mixing a solution of sodium azide (0.065g, 1 mmol) in minimum volume of aqueous methanol with constant stirring for 2 h. (10 mL). Few drops of CH_3CN were then added and the resulting mixture was additionally refluxed for 1 hour at 70°C . Finally yellow colored filtrate was kept in refrigerator for crystallization by slow evaporation. After 10 days yellow colored single crystal suitable for X-ray crystallography was obtained. Deep yellow crystals was isolated by filtration and air dried. Yield: 0.358 g (68.75%), Anal. Calc. for $\text{C}_{38}\text{H}_{40}\text{N}_{16}\text{O}_8\text{Cd}_4$: C, 35.15; H, 3.11; N, 17.26. Found: C, 35.08; H, 3.05; N, 17.30 %. IR (KBr cm^{-1}) selected bands: ν 2986 (w), 2837 (w), 2070 (vs), 1608 (vs), 1473 (s), 1217 (w) 1008 (w), 881 (w), UV-vis ($\lambda_{\text{max}}/\text{nm}$): 370 nm.

2.3.3. Synthesis of complex $[\text{Cd}_4(\text{L}^{\text{OEt}})_2(\mu_{1,1}\text{-N}_3)_3(\text{OAc})_2]$ (**2**)

To synthesize **2** similar procedure has been adopted as described for complex **1** except Schiff base ligand ($\text{H}_2\text{L}^{\text{OEt}}$) was used. The deep yellow solution was allowed to stand under freezing condition where yellow crystals were separated by filtration and was air dried. Yield: 0.236 g (63.5 %), Anal. Calc. for $\text{C}_{88}\text{H}_{102}\text{N}_{26}\text{O}_{20}\text{Cd}_8$: C, 38.53; H, 3.75; N, 13.28. Found: C, 38.47; H,

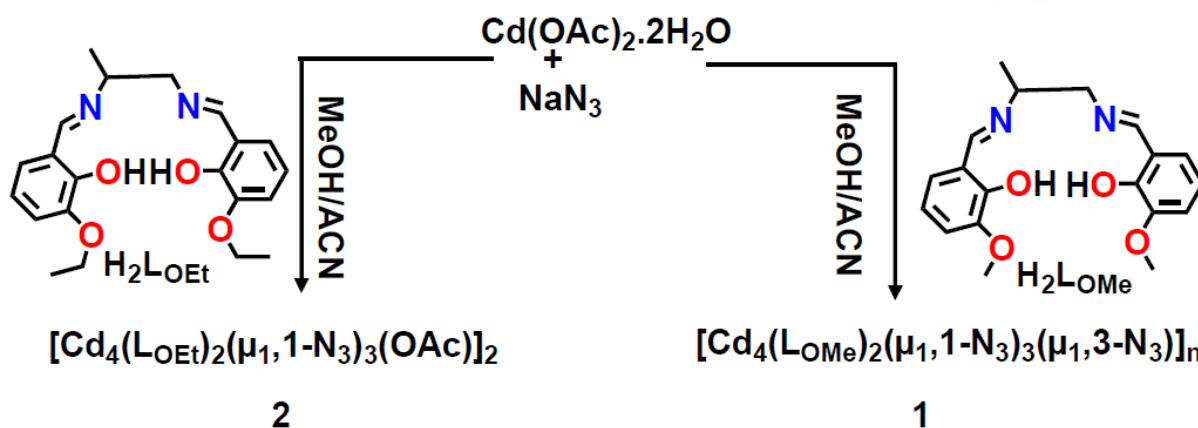
3.69; N, 13.21%. IR (KBr cm^{-1}) selected bands: ν 3792 (b), 2913 (w), 2300 (vs), 2069 (vs), 1803(vs), 1590 (vs), 1526 (w), 1329 (s), 1163 (w), 934 (w), UV-vis ($\lambda_{\text{max}}/\text{nm}$): 371 nm.

3. Results and discussion

3.1. Syntheses of Cd(II) complexes and characterizations

Less explored compartmental salen-type (N_2O_2) Schiff base ligands ($\text{H}_2\text{L}^{\text{OMe}}/\text{H}_2\text{L}^{\text{OEt}}$) are employed during complex **1** and **2** formations. Salen-type ligands formation commonly (1:2 molar ratio) belongs to condensed nature of Schiff base involving between 1,2-diaminopropane (*Pn*) and *o*-vaniline/ (OMe / OEt substituted) in methanol solvent (Generally H_2L type where H is a dissociable kind of proton). Schiff base ligands were successfully characterized by FT-IR, ^1H NMR and ^{13}C spectroscopic studies shown in Fig.S13 (see supplementary material). Both cadmium (II) complexes were derived by utilizing two close resemblance Schiff base ligands ($\text{H}_2\text{L}^{\text{OMe}}/\text{H}_2\text{L}^{\text{OEt}}$). Complex **1** and **2** were successfully synthesized by using cadmium (II) acetate dihydrate as metal precursor in methanol solution and minimum volume of water-methanol solution of sodium azide (NaN_3) were added to methanolic solution of ligands (see Scheme 2). Ligands ($\text{H}_2\text{L}^{\text{OMe}}/\text{H}_2\text{L}^{\text{OEt}}$) potentially acts as a strong compartmental hexadentate (N_2O_4) nature and thus have strong coordinating ability with Cd(II) metal centers during tetranuclear complex formation. Complex **1** is a one-dimensional polymer having azide (N_3) linkage exhibit both ($\mu_{1,1}$ end on) and ($\mu_{1,3}$ end-to-end) bridging fashion but complex **2** is a discrete octanuclear ensemble where two $[\text{Cd}_4(\text{O})_4(\text{N})_2]^{2+}$ units bridged to each other ($\mu_{1,1}$ end on end on) by ancillary azide co-ligands. Both complexes were successfully isolated only from $\text{CH}_3\text{OH}-\text{CH}_3\text{CN}$ mixed solvent medium at room temperature. Complex **1** and **2** is deep yellow colored, highly stable in air and soluble in most of the common organic solvents. Complexes were successfully characterized by different well known analytical tools like elemental analysis; UV-visible, TGA,

X-ray powder diffraction pattern, single-crystal X-ray diffraction and Fourier transform Infrared spectroscopic studies. A complete systematic characterizations approach of both Cd(II) complexes using TGA and X-ray powder diffraction pattern (PXRD) will be clearly submitted in Fig.S14 & Fig.S15(see supplementary material).



Scheme 2. Synthetic representations of tetranuclear Cd(II) complexes

Fourier transforms Infrared spectroscopy of Cd(II) complexes were analyzed and compared systematically with those of the corresponding free salen-type ligands ($\text{H}_2\text{L}^{\text{OMe}}/\text{H}_2\text{L}^{\text{OEt}}$). The FT-IR spectrum of both tetranuclear Cd(II) complexes and in related some other reported Cd(II) azide complexes were analyzed very carefully in order to predict the bridging propensity of ancillary azide co-ligand (Table S4, see Supplementary material) [68]. The appearance of strong C=N stretching value at 1630 cm^{-1} indicate positively the well-known salen-type Schiff base formation. An intense strong band at 1608 cm^{-1} and 1620 cm^{-1} for both cadmium(II) complexes is shifted considerably towards lower frequencies as compared to free ligands ($\text{H}_2\text{L}^{\text{OMe}}/\text{H}_2\text{L}^{\text{OEt}}$), that further supported coordination of binding mode of the imino nitrogen atoms of concerned ligands with the Cd(II) metal centers. Both Cd(II) complexes (**1-2**) exhibits bands near at 2070 and 2069 cm^{-1} strongly attributable to $\nu(\text{N}_3)$ binding shown in Fig.S1-S2 (see supplementary material). Additionally aliphatic C-H stretching resonances for both tetranuclear Cd(II)

complexes observed in the range 2918-2897 cm^{-1} . Finally Ar-O stretching frequencies in both Cd(II) complexes observed near at 1204-1212 cm^{-1} which is identical to the other reported salen-type ligands [69]. Thus a careful investigation of different characteristic FT-IR stretching bands for tetranuclear complexes gives an positive idea about the versatile bridging propensity of azide co-linker. The UV-Visible spectra of tetranuclear Cd(II) complexes were recorded in DMSO solvent 200-1100 nm at ambient room temperature. In DMSO solvent at room temperature Cd(II) complexes exhibits ligand-based transition at 370 & 371 nm presumably due to $\pi \rightarrow \pi^*$ or $n \rightarrow \pi^*$ transitions [70,71]. Since Cd(II) metal ion have filled d^{10} configuration hence no metal centric d-d transition was observed in complex spectrum **1** or **2**. The UV-Visible absorption spectrum of tetranuclear Cd(II) complexes (**1-2**) are clearly depicted in Fig.S3 (see Supplementary material).

4. X-ray crystal structure explanation

4.1. Crystal growth description

X-ray diffraction quality deep yellow colored single crystals have grown for both Cd(II) complexes in mixed $\text{CH}_3\text{OH}-\text{CH}_3\text{CN}$ solvent medium by slow evaporation at normal room temperature. Full Crystallographic data and detailed structural refinement parameters for tetranuclear cadmium(II) complexes (**1-2**) are clearly presented in Table S1[see supplementary material].

4.2. Crystal structure of complex $[\text{Cd}_4(\text{L}^{\text{OEt}})_2(\mu_{1,1}-\text{N}_3)_3(\text{OAc})_2]$ (**2**)

Single crystal X-ray diffraction study of **2** divulges that it is a neutral octanuclear cadmium complex $[\text{Cd}_4(\text{L}^{\text{OEt}})_2(\text{Ac})(\text{N}_3)_3]_2$ where, Ac=Acetate anion and N_3 =Azide ion. The complex **2** crystallized in the triclinic space group P-1 ($Z=1$). The perspective view of the asymmetric unit of **2** is given in the Fig.1 and selected bond parameters and bond angle are summarized in Table

S3 (see Supplementary material). From the perspective of design, the ligand $[L^{OEt}]^{2-}$ having two types of pockets which are tetradentate (O2N2) and (O4) respectively. The formation of tetranuclear assembly of asymmetric unit of **2** involves by the coordination action of the two doubly deprotonated ligands $[L^{OEt}]^{2-}$. In **2** each of the two $[L^{OEt}]^{2-}$ binds to four cadmium metal ions. Interestingly utilizing tetradentate pocket (O2N2) accommodate only one Cd(II) ion. On contrary, other tetradentate pocket (O4) housing three Cd(II) ions at a time utilizing bridging μ_3 -oxygen atom and bridging μ_2 -oxygen atom. Apart from the binding action provide by the $[L^{OEt}]^{2-}$ the tetranuclear framework is further strengthened by the two bridging $\mu_{1,1}$ -N₃⁻ groups. Besides this, one acetate ion attached to one of the terminal Cd(II) ion in η^2 -OAc fashion to neutralize the overall charge of the complex in Fig.S5 (see supplementary material). A close inspection reveals that the asymmetric units of **2** further grow at the azide bridging (N8-N9-N10) to give the overall a homometallic octanuclear ensemble. The coordination modes of the ligands involved in the assembly of **2** are given in Fig.2. Further investigation of the crystal structure of **2** reveals that the μ_3 -oxygen, μ_2 -oxygen of the ligand $[L^{OEt}]^{2-}$ and μ_2 -azide leads to the dicationic tetranuclear core $[Cd_4(O)_4(N)_2]^{2+}$ featuring a butterfly shaped topology (see Fig.3) [72,73]. The butterfly shaped Cd₄ core is consist of four cadmium metal ions; Cd2 and Cd3 represents the body where as Cd1 and Cd4 represents the wing. Among the four cadmium metal ions the metal ions Cd1 and Cd4 are six coordinated and contain a 5O, 1N and 3O, 3N coordination environment respectively with a trigonal prismatic structure where as Cd2 and Cd3 are seven coordinated and both contain a 4O, 3N coordination environment with square face monocapped in Fig.S6 (see supplementary material). The Cd-O bond distance fall in the following range, the average Cd-O_{Et}=2.465Å and Cd- μ_3 O =2.379Å and Cd- μ_2 O =2.256Å and Cd-N bond distance fall in the range 2.329-2.342(9) Å with the small bond distance for Cd- $\mu_{1,1}$ -

N_3 (average ~ 2.289). The Cd-O-Cd and Cd-N-Cd bond angles in compound **2** are in the range 98.108 (2) -103.11 (2). All the bond distances and bond angles are similar and are comparable to found in the literature (Table S5, see supplementary material) [74].

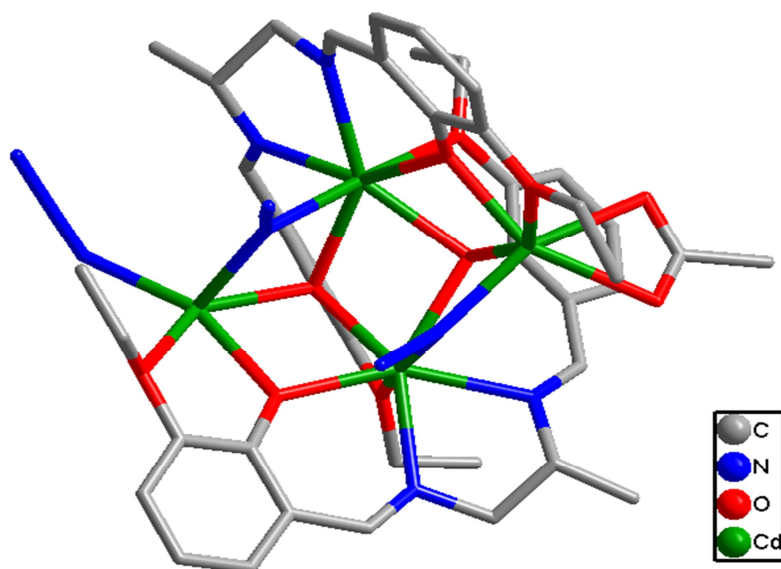


Fig.1. The perspective view of the asymmetric unit of complex **2**

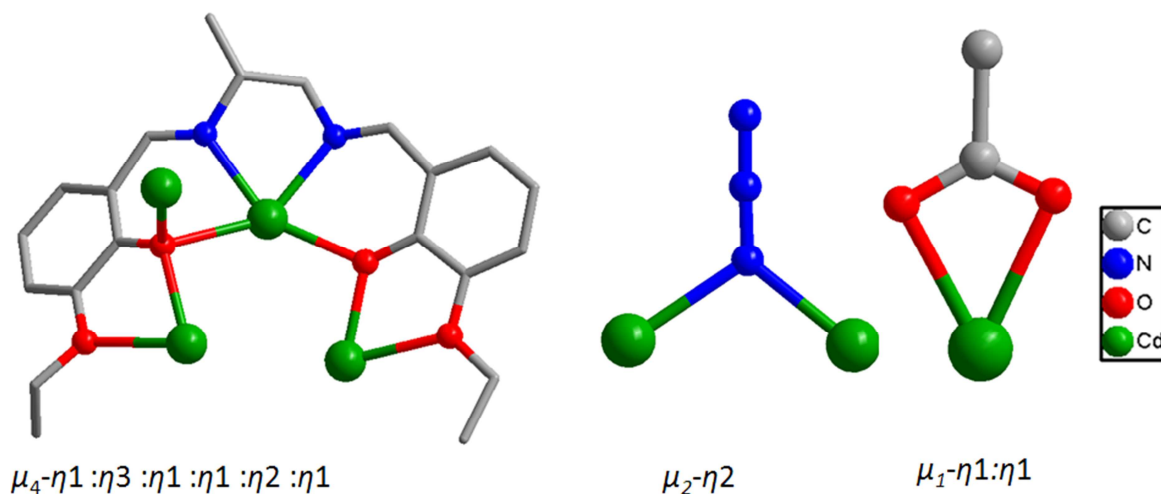


Fig.2. Bindings mode of ligand $[L^{OEt}]^{2-}$, azido and acetate anion

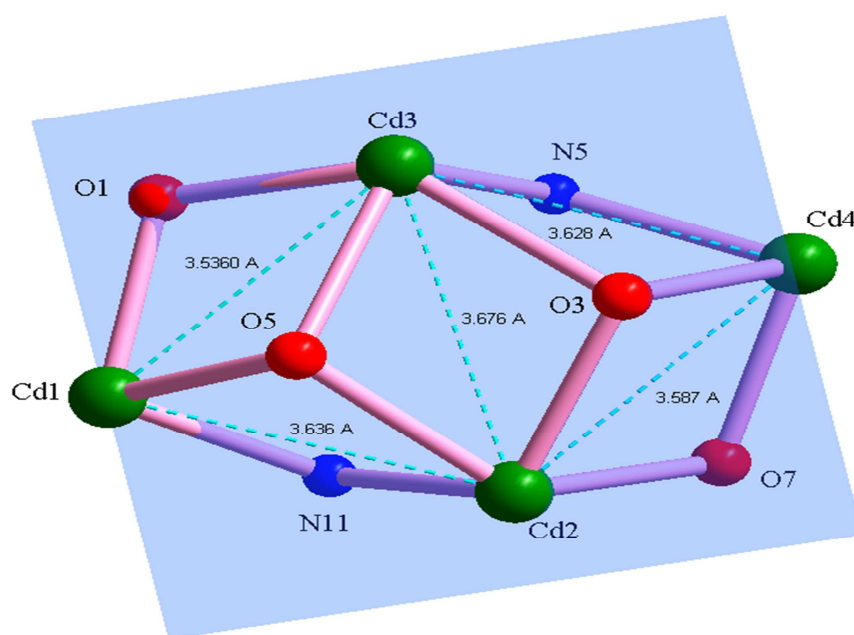


Fig.3. Butterfly shaped tetrameric core in complex **2**

4.3. Crystal structure of complex $[\text{Cd}_4(\text{L}^{\text{OMe}})_2(\mu_{1,1}\text{-N}_3)_3(\mu_{1,3}\text{-N}_3)]_n$ (**1**)

Crystallographic investigation of complex **1** reveals that the asymmetric unit contains four crystallographic independent cadmium metal ions and it is a neutral tetranuclear complex $[\text{Cd}_4(\text{L}^{\text{OMe}})_2(\text{N}_3)_4]$ where, $\text{N}_3 = \text{Azide}$. Compound **1** crystallizes in the monoclinic space group $P2_1/n$ ($Z=4$). The asymmetric unit **1** is given in the Fig.S7 (see supplementary material) and selected bond parameters are summarized in Table S2 (see Supplementary material). Like $\text{H}_2\text{L}^{\text{OEt}}$, the ligand $(\text{H}_2\text{L}^{\text{OMe}})$ having two unsymmetrical tetradentate pockets comprised of O2N2 and O4 coordination sphere. The formation of tetranuclear assembly of asymmetric unit of **1** involves by the cumulative coordination action of the two doubly deprotonated ligands $[\text{L}^{\text{OMe}}]^{2-}$. Two of such doubly deprotonated ligands binds to the four cadmium metal ions by using their above-mentioned pockets. Besides this the asymmetric unit is further strengthened by the two

bridging $\mu_{1,1}\text{-N}_3^-$ groups. Two tetranuclear asymmetric unit joins to its adjacent unit by two equivalent end-on $[\text{N}_3]^-$ coligands which are bridging between two symmetrically generated Cd4 atoms forming an octanuclear ensemble $[\text{Cd}_4(\text{L}^{\text{OMe}})_2(\text{N}_3)_4]_2$ (see Fig.3). It is exactly showing resemblance to the structure of **2**. Further investigation on **1** reveals that each octanuclear building unit are linked to each other by means of two *trans* end-to-end (EE $\mu\text{-1,3}$) $[\text{N}_3]^-$ coligands which actually bridging between two symmetrically generated Cd1 atoms forming a one-dimensional polymeric chain. Here it is interesting to mention that there is an existence of eight membered ring (Cd_2N_6) which is unlikely stabilized in chair conformation due to *trans* end-to-end (EE $\mu\text{-1,3}$) binding of linear azido ligands in Fig.S8 (see supplementary material). Perhaps due to presence of more flexible $\text{-CH}_2\text{-CH}_3$ moiety in **1** creates steric effect and oppose to the formation of such chair conformation arrangement. It is interesting to note that unlike **2** the **1** is a 1D polymeric structure. Perhaps due to presence of more flexible $\text{-CH}_2\text{-CH}_3$ moiety in **1** creates steric effect and oppose to the formation of such chair conformation arrangement. It is interesting to note that unlike **2** the **1** is a 1D polymeric structure. Although both the crystal structure of **2** and **1** contain $\text{C-H}\cdots\pi$ but the H atom of the different group involving in $\text{C-H}\cdots\pi$ are different in Fig.S4 (see supplementary material). The different coordination modes of ligands present in **1** are given in Fig.4. Out of four cadmium metal ions the Cd1 and Cd4 are six coordinate both having 3O, 3N coordination environment with an octahedral arrangement for the Cd1 and trigonal prismatic for Cd4 metal ion. The metal ions Cd2 and Cd3 are seven coordinated and both contain 4O, 3N coordination environment with square face monocapped geometry (see Fig.5). The Cd-O bond distance fall in the range 2.235(4)-2.503(4) and Cd-N bond distance 2.242(5)- 2.364(6) Å. All the bond distance and bond angles are similar and are comparable to found in the literature TableS5 (see supplementary material) [74]. To enhance the broad

coordination chemistry knowledge of structurally characterized tetranuclear Cd(II)-azido bridged complexes in presence of current investigated ligands (H_2L^{OMe}/H_2L^{OEt}), we have also explored the coordination chemistry in details involving very close resemblance ligands in the same field as a concise comparative manner. Apart from, in Table S6 (see supplementary material) [75] we have also clearly focused on the importance of M^{II} chemistry [M^{II} =bivalent metal other than Cd metal ions] involving identical salen-type ligands with reference to ligand potential donor centers, azide bridging versatility etc.

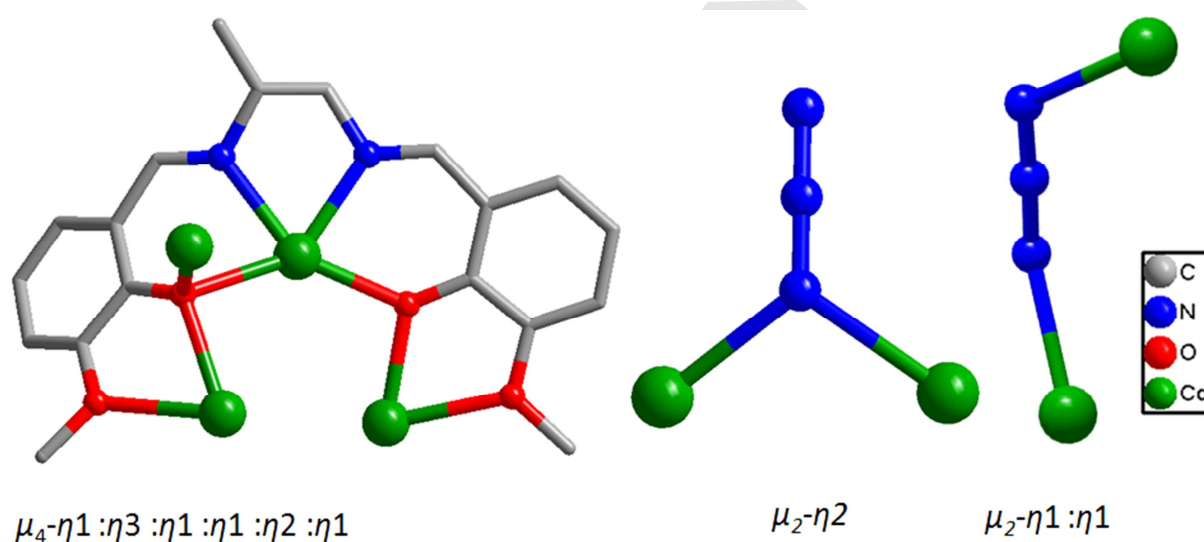


Fig.4. Bindings mode of ligand $[L_1]^{2-}$ and azide ion

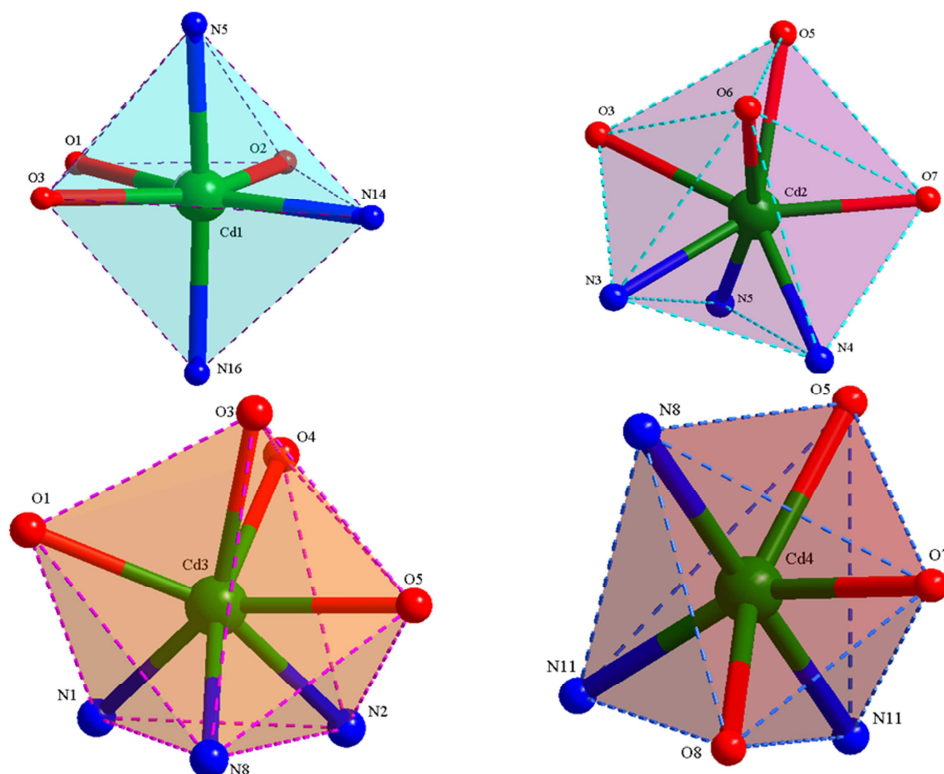


Fig.5. Metal coordination geometry in complex **1**

5. Computational DFT approach

5.1. Frontier molecular orbital analysis

The frontier molecular orbitals, HOMO and LUMO and their energy values gives an indication of the approximate chemical reactivity and kinetic stability of tetranuclear Cd(II) complexes. The HOMO-LUMO analysis was carried out on the DFT optimized structures and on analysis it was found that the energy gap is comparable but highest on **2** with a difference of about 0.286 eV in Fig.S9 (see supplementary material). From the HOMO-LUMO energy values the global reactivity descriptors can be predicted in Table S7 [see supplementary material]. Orbital compositional analysis was carried out on the frontier orbitals which returned interesting results.

On performing orbital compositional analysis using Mulliken method it was found that for **1**, HOMO is mainly centered on two benzenoid rings with a contribution of 21.79% and 35.22% (π type) (one from each ligand unit) and also from the associated phenoxo and methoxy oxygen atoms 25.29% (p type) and azide coligands (14.49%, p type) with metal having no contribution whatsoever. In the case of LUMO both the metal centres and azide coligands have no contribution and the azomethine groups contribute heavily with a cumulative contribution of about 48.729 % followed by the benzenoid rings of the ligand units with 39.88% (π^* type). In the case of **2**, similar to the case of **1** no contribution from the metal centres were found and here only one of the ligand contributes with the benzenoid rings with a share of 58.35% (π type). This is followed by the associated phenoxo and ethoxy oxygen atoms 25.21%, azomethine nitrogen atom 3.22% (p type) from the same ligand. All the azide coligands have some minor share with a cumulative value of about 4.408%. The LUMO contribution comes from the ligand unit which had no share in HOMO. The azomethine groups in the ligand have the highest share (78.14%) followed by the benzenoid rings which gives a cumulative contribution of about 18.63% (π^* type). Due to the similarity in solid state structures similar results were obtained for both the complexes on performing Mulliken charge analysis. It was found that the highest positive charge is concentrated on the four Cd metal centers in both the complexes ranging from +0.92 to +1.5. Oxygen donor atoms have the highest negative charge with phenoxo type in the range -0.71 to -0.74 for both complexes while that of the methoxy type falls in the range -0.55 to -0.57 (-0.58 to -0.45 in **2**). The azide co-ligands closely follow with the charges ranging from -0.65 to -0.28 (highest for the bonded and least for the middle one) (-0.67 to -0.38 in **2**). The coordinated donor azomethine nitrogen atoms have a consistent value ranging from -0.44 to -0.41 (-0.428 to -0.435 in **2**).

5.2. Electrostatic potential maps (ESP) analysis

The electrostatic potential maps (ESP) were generated on DFT optimized structures at B3LYP/def2-TZVP level of theory to visualize electrophilic and nucleophilic regions in the molecule (see Fig 6). The red regions reveal the areas prone to nucleophilic attack while blue electrophilic ones undergo attacks. Owing to the similarity in their structures both the complexes **1** and **2** have similar solid state architectures and exhibit the same type of hydrogen bonding interactions. This is also reflected in their molecular electrostatic potential maps whereby both the complexes show comparable minimum and maximum values. From the crystal structure analysis it is clear that both the complexes exhibit non-classical intramolecular hydrogen bonding interactions with methoxy carbon as the donor and azide nitrogen as the acceptor. This is further evidenced from ESPs where both the complexes showed a positive potential (+9 kcal/mol for complex **1** and +11 kcal/mol for complex **2**) in the proximity of the methoxy carbon bound hydrogen (C35-H35B in complex **1** and C39-H39A in complex **2**) and a negative potential near azide nitrogen (N12 in complex **1** and N6 in complex **2**) (-38 kcal/mol in complex **1** and -42 kcal/mol in complex **2**). Also in complex **1**, the centroid Cg(5) comprising of atoms C1 to C6 is at a negative potential (π -basic ring) of about -11 kcal/mol which justifies its CH $\cdots\pi$ interaction with methoxy carbon bound hydrogen H35A (+25 kcal/mol). Similarly in complex **2**, Cg(4) comprising of atoms C12 to C17 which is at a negative potential of about -15 kcal/mol interacts with ethoxy bound hydrogen (H39C (+23 kcal/mol)) of adjacent molecule. The trend for the highest positive and negative potentials is again similar on both the complexes and in line with the reported complexes with the highest positive potentials seen near the azomethine bound hydrogen (NH), spacer diimine group (+30 to +47 kcal/mol) [76] and the highest negative

potentials are seen near azide coligands (with regions near terminal N atoms reaching up to -48 kcal/mol).

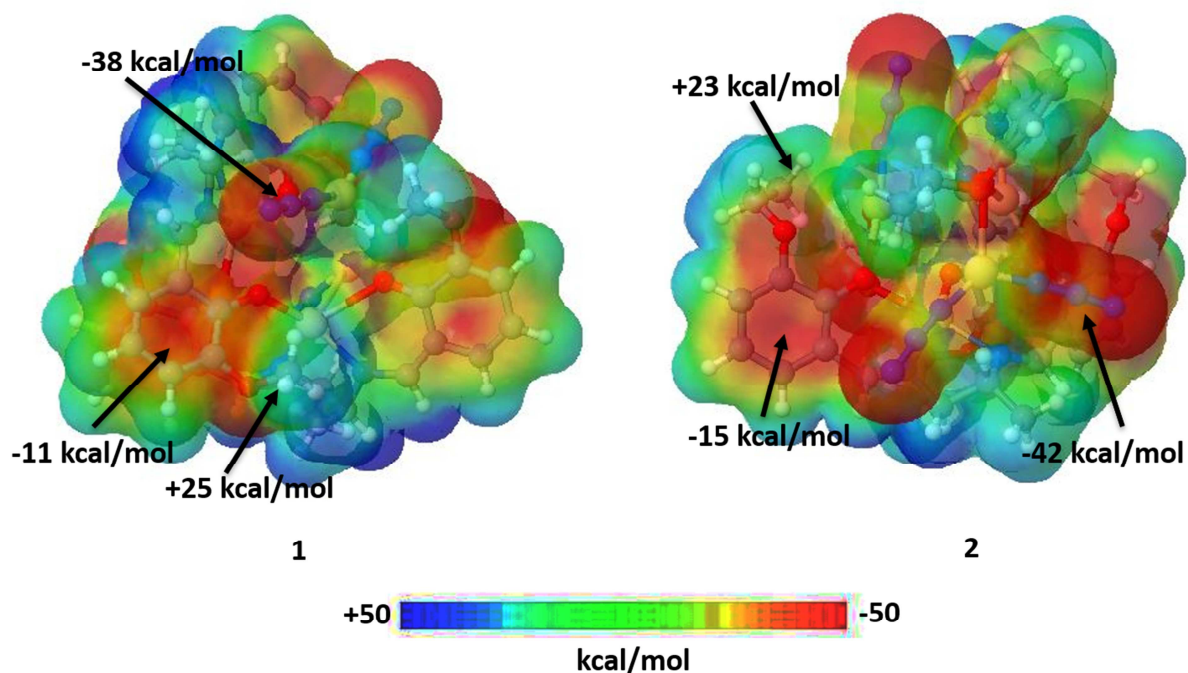


Fig.6. Electrostatic potential map of complex **1** and complex **2** on electron density isosurface computed at the B3LYP/def2-TZVP level of theory.

6. Computational TD-DFT analysis

The TD-DFT study of tetranuclear azido-bridged Cd(II) complexes exhibits electronic transitions which are mainly due to intra-ligand charge transfer. The calculated absorption maxima in Figure S10 black color (see supplementary material) arises at 354.13 nm for complex **1** (Experimental ~370 nm) with oscillator strength, $f = 0.0945$. HOMO-1 mainly consists of ligand π -orbitals and very small contribution from metal d orbital and HOMO-2 is consists of ligand π -orbitals only. Whereas the LUMO and LUMO+1 are consist of ligand π^* -orbitals only. In case of complex **2**, it shows calculated peak in Figure S10 red color (see supplementary material) at 359.22 nm

(Experimental ~371 nm) arises mainly due to intra-ligand transitions with oscillator strength, $f = 0.1586$. TD-DFT related all orbital electronic transitions are clearly shown in Table S8 [see supplementary material]. All the MOs generated in connection of TD-DFT calculations of Cd(II) complexes are lucidly presented in Figure S10 [see supplementary material].

7. Photo physical properties of Cd(II) complexes

Fluorescence behavior of salen-type Schiff base ligands (H_2L^{OMe}/H_2L^{OEt}) and tetranuclear complexes (**1-2**) were recorded in DMSO solvent at room temperature in Table 1 and the ligand centered emission spectra are compared in Fig.7 revealing that ligands are practically non-emissive but the Cd(II) complexes exhibit strong fluorescent behavior. Upon photo excitation at 333 nm, Schiff base Ligands (H_2L^{OMe}/H_2L^{OEt}) exhibits a fluorescent emission centered at 500 and 501 nm. Cd(II) complexes (**1-2**) upon photo excitation at wavelength 372 & 373 nm shows photoluminescence with the main emission peak at 519 & 516 nm. The emission bands for complex **1** and **2** are nearly similar to those of the other reported Cd(II) complexes (Table S9, see supplementary material) [77]. For complexes (**1-2**), no emission emanating from metal-centered MLCT/LMCT excited states are possible since it is hard to oxidize or reduce d^{10} configuration Cd(II) metal ion. The photo luminescent emission nature of Cd(II) metal complexes (**1-2**) may therefore be assigned mainly due to the L→M charge transfer. As a common popular knowledge of fluorescence chemistry, the enhancement of the emission intensities of (**1-2**) may be due to the metal ligand chelation effect [78-81] or most probably the increase in conformational rigidity of salen-type ligands (H_2L^{OMe}/H_2L^{OEt}) chelation imparted via N, O-donor center with Cd(II) metal [78,79]. Now at the time of metal binding process with N,O-donor ligand, non-radiative channels and flexible bonds are inactive due to strong binding. This well known phenomenon popularly referred as 'CHEF EFFECT' which has been mainly reported in d^{10} configuration metal ions viz.

Cd(II)/Zn(II)/Hg(II) especially those containing organic backbone fused ring structures involving nitrogen or oxygen potential donor centers. Thus the enhancement of fluorescence phenomenon through stable chelate complex formation in presence of salen-type ligands is more interesting and attractive as it opens up the new avenue of opportunity for different photochemical applications of these complexes [81]. A closer inspection of salen-type ligands (H_2L^{OMe}/H_2L^{OEt}) divulges that identical absorption and emission maxima spectra have been observed for ligands containing a methoxy/ethoxy group in ortho position of the phenol moiety [82]. Further, reported Schiff base ligands (H_2L^{OMe}/H_2L^{OEt}) quantum yield (ϕ) values are very low which are nearly identical to other reported Schiff base ligands (H_2L^{OEt}) [N,N'-bis(3-ethoxysalicylideneimino)-1,3-diaminopropane] (4.6×10^{-3}), (H_2L^0) [N,N'-bis(salicylidene)-1,3-diaminopentane] (9.3×10^{-3}) as well as Schiff base (H_2L^{OMe}) [N,N'-bis(3-methoxysalicylideneimino)-1,3-diaminopropane] (8.9×10^{-3}) [83,84]. The quantum yield (Φ) values comparison of synthesized Cd(II) complexes (**1-2**) with other reported cadmium complexes are nearly identical and shown in Table 2 as a concise supporting evidence [85].

Table 1 Photo-physical parameters of Schiff base ligands (H_2L^{OMe}/H_2L^{OEt}) and tetranuclear Cd(II) complexes in DMSO at room temperature (298 K)

Compound	Absorption (λ_{max}), nm	Excitation (λ_{max}), nm	Emission (λ_{max}), nm
Ligand(H_2L^{OMe})	264, 332, 427	333	500
Ligand(H_2L^{OEt})	264, 333, 427	333	501
Cd ^{II} complex (1)	285, 372	372	519
Cd ^{II} complex (2)	285, 373	373	516

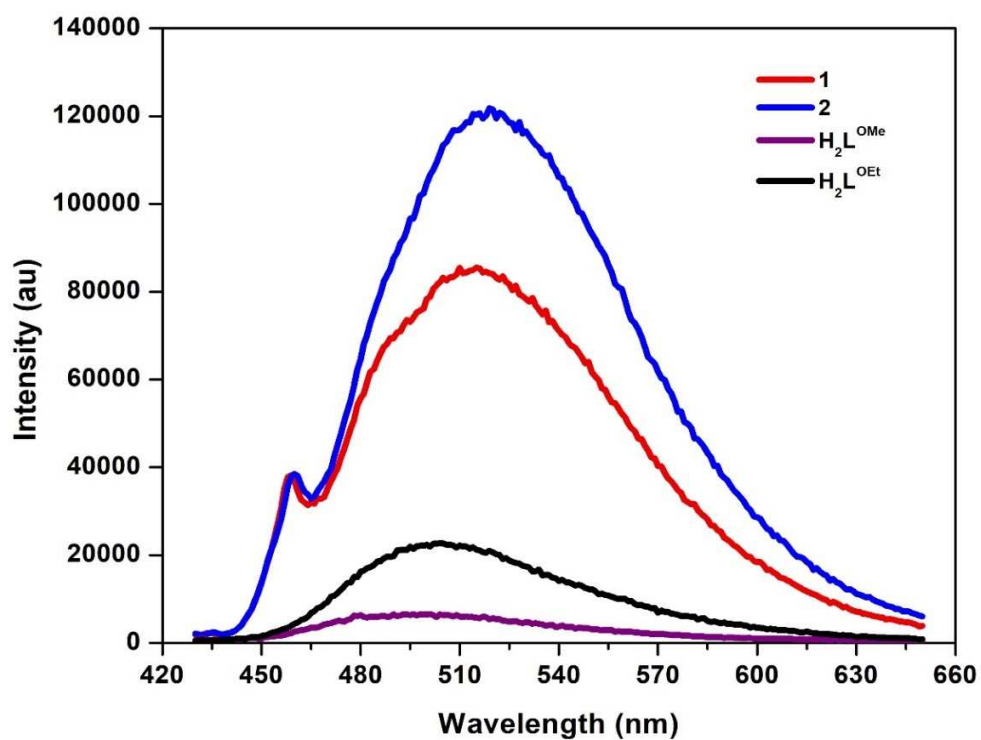


Fig. 7. Ligand centered emission spectra of ligands ($\text{H}_2\text{L}^{\text{OMe}}/\text{H}_2\text{L}^{\text{OEt}}$) and tetranuclear Cd(II) complexes in DMSO at 298K

Table 2 Quantum yield (Φ) values comparison of salen-type ligands, tetranuclear Cd(II) complexes and other reported important cadmium(II) complexes

Compounds	Quantum yield (Φ)	References
Schiff base(HL ^{OMe})	0.00353,	This work
Schiff base(HL ^{OEt})	0.01308	This work
Identical Schiff base(H ₂ L ^{OEt})	4.6x10 ⁻³	a
Identical Schiff base (H ₂ L ^{OMe})	8.9x10 ⁻³	b
Identical Schiff base (H ₂ L ⁰)	9.3x10 ⁻³	c
[Cd ₂ L ^{OMe} ($\mu_{1,1}$ -N ₃)($\mu_{1,3}$ -N ₃) _n (1)	0.02742	This work
[Cd ₄ (L ^{OEt}) ₂ ($\mu_{1,1}$ -N ₃) ₃ (OAc)] ₂	0.02872	This work
[Cd ₄ (L ^{OEt}) ₂ ($\mu_{1,1}$ -N ₃) ₃ (η^1 -N ₃) ₂	0.03767	d
[Cd ₄ (N ₃) ₄ (L ¹).H ₂ O] _n	0.03410	e
[Cd(N ₃)(NO ₃)(terpy)(H ₂ O)]	<0.1	f
[Cd ₂ ($\mu_{1,1}$ -N ₃) ₂ (N ₃) ₂ (terpy) ₂]	<0.1	f
[Cd ₃ ^{II} (N ₃) ₄ (L ²) ₂] _n	0.0236	g
[Cd ₂ ^{II} (N ₃) ₃ (L ¹) _n	0.0067	
[Cd ₄ (SCN) ₄ (L ¹) ₂] _n	0.0370	h
[Cd ₂ (L ²) ₂ (SCN) ₂ (CH ₃ OH)]	0.0330	i
[Cd ₂ (L ³) ₂ (NO ₃) ₂]	0.03219	j

8. Antibacterial and anti-biofilm properties of cadmium (II) complexes

Two Cd(II) complexes and respective salen-type Schiff base ligands (H_2L^{OMe}/H_2L^{OEt}) exhibited antibacterial potency against the four selected bacterial strains. The MIC values of the complexes, Schiff base ligands and their growth inhibition zone diameters for the tested bacterial strains are clearly submitted in Table 3A. In this context some reported Cd(II) Schiff base complexes and cadmium salts (MIC/GIC) possible values against tested some important bacterial stains will also be highlighted in Table 3B to emphasize better comparison of our synthesized Cd(II) complexes antibacterial results [86a-j]. Both the complexes had the lower MIC ($\mu\text{g/mL}$) values compared to their respective ligands implying greater antimicrobial efficiencies. On the other hand, those complexes and ligands had lower MIC against both Gram negative bacterial strains than those for Gram positive bacterial strains. It suggests that Gram negative bacteria are more susceptible to be affected by those chemicals. Cd(II)-azido complexes (**1** and **2**) showed higher growth inhibition zone diameter (mm) than the free salen-type ligands (H_2L^{OMe}/H_2L^{OEt}) which also conform to their MIC values. All the complexes (**1-2**) and Schiff base ligands had higher growth inhibition zone diameter against both Gram negative bacterial strains than the Gram positive bacterial strains. There appeared a distinct variation in MIC and growth inhibition zone diameter of the complexes and ligands which in the following order: complex **2** \geq complex **1** $>$ $H_2L^{OEt} \geq H_2L^{OMe}$ (LSD test; $P < 0.05$).

Bacterial growth was inhibited by both Cd(II) complexes but in case of the ligands (H_2L^{OMe}/H_2L^{OEt}) bacterial growth inhibition was very low at their MIC against both tested bacterial strains. Time-kill curves of the selected bacterial strains (*E. gallinarum* and *P. vulgaris*) subjected to the complexes (**1-2**) are showed in Fig.8. They reflected distinct treatment differences (LSD test; $P < 0.05$) in the inhibition pattern of bacterial growth in the following

order: complex **2** \geq complex **1** $>$ $\text{H}_2\text{L}^{\text{OEt}} \geq \text{H}_2\text{L}^{\text{OMe}}$. While subjected to the complexes (**1-2**), *P. vulgaris* exhibited gradually decreasing trend of growth all through although at a slower rate. In contrast the bacteria showed gradual increase in growth rate although remaining much lower than the growth without having any chemical entities. For *E. gallinarum* showed a slight rate of increase up to 90 min followed by a gradually decreasing trend in presence of the complex **1** and complex **2** with an overall decline of growth by 77 and 84% respectively. While subjected to the salen-type ligands ($\text{H}_2\text{L}^{\text{OMe}}/\text{H}_2\text{L}^{\text{OEt}}$), the bacterial growth increased gradually but remained lower than the control registering an overall decrease in growth by 18 and 21% for ($\text{H}_2\text{L}^{\text{OMe}}$) and ($\text{H}_2\text{L}^{\text{OEt}}$) respectively. Contrarily, complexes (**1** and **2**) induced great effects in retarding growth of *P. vulgaris* from the very beginning to the end of the incubation period (210 min). Consequently the bacteria exhibited a continuously declining growth pattern registering overall decline of growth by 91 and 98% respectively. In presence of ligands ($\text{H}_2\text{L}^{\text{OMe}}/\text{H}_2\text{L}^{\text{OEt}}$) although the growth rate of *P. vulgaris* was reduced compared to the control but the bacteria showed a gradual increasing trend similar to *E. gallinarum* with a resultant decrease to the tune of 30 and 41% respectively.

The study on biofilm removal efficiency of Cd(II) complexes (**1-2**) and their Schiff base ligands ($\text{H}_2\text{L}^{\text{OMe}}/\text{H}_2\text{L}^{\text{OEt}}$) against *E. gallinarum* and *P. vulgaris* are clearly presented in Fig.S11 (see supplementary material) showed that all the tested chemicals were proved more effective in removal of biofilm produced by Gram negative bacteria (*P. vulgaris*) compared to that of Gram positive bacteria (*E. gallinarum*). Both complexes (**1-2**) exerted greater biofilm removal efficiency compared to their corresponding ligands ($\text{H}_2\text{L}^{\text{OMe}}/\text{H}_2\text{L}^{\text{OEt}}$). Complex **2** exhibited the highest biofilm removal efficiency against both tested strains. In both complexation, there

appeared a significant variation in biofilm removal efficiency of the Cd(II) complexes and ligands in the following order: complex **2** > complex **1** > H_2L^{OEt} > H_2L^{OMe} (LSD test; $P < 0.05$).

The results of MTT assay of the chemical entities against *E. gallinarum* and *P. vulgaris* in Fig.S12 (see supplementary material) showed that the complexes (**1-2**) were more effective than ligands (H_2L^{OMe}/H_2L^{OEt}). Cell mortality percentage was also higher in case of Gram negative bacterial strain than the Gram positive bacterial strain which has a significant implication for their potential use as candidates against pathogenic bacteria in general, and Gram negative bacteria in particular. Chemicals showed distinct variations in inflicting cell mortality in the following order: complex **2** > complex **1** > H_2L^{OEt} > H_2L^{OMe} (LSD test; $P < 0.05$). Membrane damage assay of *E. gallinarum* and *P. vulgaris* in presence of the both tetranuclear Cd(II) complexes and Schiff base ligands are shown in Fig.9. Both Cd(II)-azido bridged complexes (**1-2**) offered an encouraging efficiency to damage bacterial cell membrane compared to the Schiff base ligands (H_2L^{OEt} and H_2L^{OMe}). All the complexes and ligands (H_2L^{OEt} and H_2L^{OMe}) were more effective on Gram negative bacterial membrane (*P. vulgaris*) compared to that of Gram positive bacterial membrane (*E. gallinarum*). It reflected distinct treatment differences (LSD test; $P < 0.05$) in the release amount of nucleic acids subject to the complexes in the following order: complex **2** > complex **1** > H_2L^{OEt} > H_2L^{OMe} . The observed biological activities of both tetranuclear Cd(II) complexes are nearly similar with other reported cadmium(II) azide complexes shown in Table S10 (see Supplementary material) [87].

Table 3A MIC ($\mu\text{g/mL}$) and bacterial growth inhibition zone diameter (mm) against the complexes (**1** and **2**) and the ligands ($\text{H}_2\text{L}^{\text{OMe}}/\text{H}_2\text{L}^{\text{OEt}}$) of the tested bacterial strains.

Bacteria	Complex 1=S1		Complex 2=S2		$\text{H}_2\text{L}^{\text{OMe}} = \text{L1}$		$\text{H}_2\text{L}^{\text{OEt}} = \text{L2}$	
	MIC	Growth inhibition zone (mm)	MIC	Growth inhibition zone (mm)	MIC	Growth inhibition zone (mm)	MIC	Growth inhibition zone (mm)
<i>B. subtilis</i>	58	9.89 \pm 0.55	54	10.62 \pm 0.91	550	4.13 \pm 0.28	500	4.35 \pm 0.51
<i>E. gallinarum</i>	54	11.37 \pm 0.83	42	12.29 \pm 0.74	500	5.89 \pm 0.31	450	5.13 \pm 0.62
<i>P. vulgaris</i>	46	12.81 \pm 0.59	40	13.48 \pm 0.62	350	7.94 \pm 0.22	300	8.29 \pm 0.42
<i>E. aerogenes</i>	52	10.51 \pm 0.43	38	12.84 \pm 0.59	450	6.67 \pm 0.41	400	7.68 \pm 0.19

Table 3B MIC ($\mu\text{g/mL}$) and bacterial growth inhibition zone diameter [GIC] (mm) against some important reported Cd(II) Schiff base complexes tested bacterial Strains

Bacteria	<i>B. subtilis</i>		<i>E. gallin m</i>		<i>P. vulgaris</i>		<i>E. aerogenes</i>		Ref
Complexes	MIC	GIC (mm)	MIC	GIC (mm)	MIC	GIC (mm)	MIC	GIC (mm)	
$\{[\text{Cd}_4(\text{N}_3)_4(\text{L1})_2] \cdot (\text{H}_2\text{O})_n\}$	30	8.4	-	-	30	7.8	140	5.8	a
$[\text{Cd}_4(\text{SCN})_4(\text{L1})_2]_n$	20	7.3	-	-	20	8.8	140	6.5	

[Cd(valp) ₂ (imidazole) ₂]	10	100%					10	60-70%	b
[Cd(valp) ₂ (phen)H ₂ O]	15	60-70%					15		
[CdL ₂](ClO ₄) ₂	-	-	>128	-	-	-	0.78	-	c
[Cd(L)Br ₂]			>128				25		
[Cd ₂ (L) ₂ (NO ₃) ₄]			>128				6.25		
[Cd ₂ (L) ₂ I ₄],			>128				1.56		
CdLCI ₂	125	28.20	-	-	-	-	-	-	d
CdLBr ₂	37	28.00							
CdLI ₂	125	25.30							
CdL(NCS) ₂	125	27.42							
[Cd(NS) ₂]	50,00 0	19					781	²⁰	e
[Cd(MP _z OATA)Cl ₂] ₂	40	5.5±0.3	-	-	35	3.8±02	175	5.5±0.3	f
[CdL ¹ (ClO ₄) ₂]CH ₃ CN	4	50±5	-	-	-	-	-	-	g

Table 3B MIC (µg/mL)/GIC of some important Cadmium salts against tested bacterial Strains

Bacteria	<i>B.Cereus</i>	<i>S.aureus</i>	<i>S.typi</i>	<i>P.aeruginosa</i>	<i>E.coli</i>	<i>B.subtilis</i>	<i>C.albicans</i>	Ref
								86
Cd(ClO ₄) ₂	10	8	8	7	-	-	-	h
Cd(NO ₃) ₂	-	125	500	>1000			62.5	i
CdSO ₄	-	125	500	>1000	-	-	62.5	i

CdCl ₂	-	62.5	125	500	-	-	62.5	i	
CdI ₂	42	39	38	-	35	-	-	i	
		MIC	GIC		MIC	GIC	MIC	GIC	
Cd(OAc) ₂		-	-		6.25	35	3.12	40	j

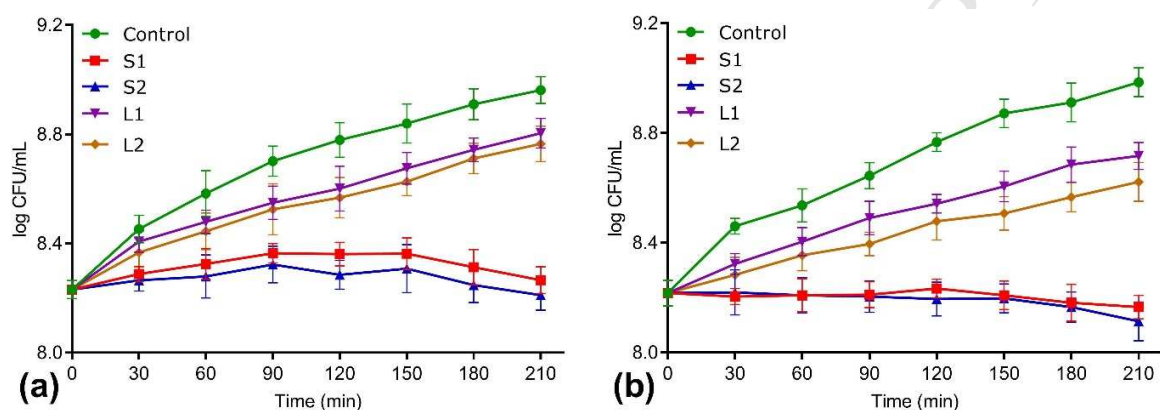


Fig.8. Time-kill curves of (a) *E. gallinarum* and (b) *P. vulgaris* against the Cd (II) complexes (**1** and **2**) and the ligands (H_2L^{OMe}/H_2L^{OEt}). All data were taken in triplicate and error bars shows standard deviation

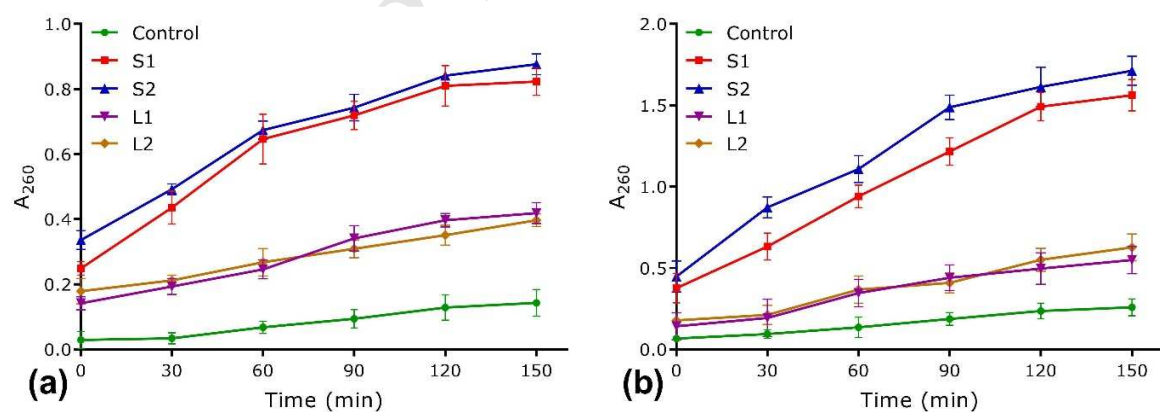


Fig.9. Membrane damage efficiency of the complexes (**1** and **2**) and the ligands (H_2L^{OMe}/H_2L^{OEt}) against (a) *E. gallinarum* and (b) *P. vulgaris*

9. Conclusion

Two novel tetranuclear cadmium(II) polymeric and discrete complexes viz, $[\text{Cd}_4(\text{L}^{\text{OMe}})_2(\mu_{1,1}\text{-N}_3)_3(\mu_{1,3}\text{-N}_3)]_n$ (**1**) and $[\text{Cd}_4(\text{L}^{\text{OEt}})_2(\mu_{1,1}\text{-N}_3)_3(\text{OAc})]_2$ (**2**) have been synthesized in presence of closely identical N,O-donor salen-type Schiff base ligands ($\text{H}_2\text{L}^{\text{OMe}}/\text{H}_2\text{L}^{\text{OEt}}$) and structurally well characterized. As a consequence of minor changes in the substituent from OMe to OEt in the benzene ring of salen-type ligands ($\text{H}_2\text{L}^{\text{OMe}}/\text{H}_2\text{L}^{\text{OEt}}$), the complexes exhibit different topologies of their azide bridging sequences. The excellent bridging propensity of azide (N_3^-) as counter ions in both Cd(II) complexes is strongly reflected by their marvelous bridging fashion ($\mu_{1,1}$ end on) and ($\mu_{1,3}$ end-to-end). Critically, Ligand-based fluorescence, quantum yield, thermal behavior of two novel Cd(II) polymeric-discrete complexes have also been discussed. Complex **1** and **2** exhibits strong luminescent emissions which are tuned mainly by the ligand based photoluminescence. The enhanced luminescence behavior of cadmium (II) complexes further to be promoted as a strong photoactive material. Thermo gravimetric analyses have been performed for complex **1** and **2** in order to investigate mainly for the thermal stability of metal-organic frameworks present in the complexes. Complex **1** and **2** exhibited strong antibacterial and anti-biofilm activities against some important Gram +ve and Gram -ve bacterial strains implying their prospective use as bacteriostatic and/or anti-biofilm agents.

Acknowledgements

This research work did not receive any specific grant from funding agencies in the public, commercial or not-profit sectors. Dr. Dipankar Mishra gratefully acknowledges the financial grant sanctioned by UGC, New Delhi, in his favour vide Minor Research Project (F.PSW-232/15-16(ERO)). Dr. Sourav Das acknowledges support from Early Career Research Award Grant from Science and Engineering Research Board (SERB), India (Project File

no.ECR/2016/001746). Dr. Dhiraj Das also thanks to Dr. Angshuman Roy Choudhury and IISER Mohali for taking up the facility of Gaussian 09 software.

Appendix A. Supplementary material

Details supplementary data related to this article can be associated in ESM. CCDC number 1811084-1811085 contains the supplementary crystallographic data (excluding structure factors) in CIF format for the structure reported of tetranuclear Cd(II) complexes. Copies of the data can be obtained, free of charge, on application to CCDC, 12 Union Road, Cambridge CB2 1EZ, U.K.: <http://www.ccdc.cam.ac.uk/cgi-bin/catreq.cgi>, e-mail: data_request@ccdc.cam.ac.uk, or fax: +44 1223 336033

References

- [1] B. Xiao, H. Hou, Y. Fan, M. Tang, Impact of counteranion on the self-assembly of Cd(II)-containing MOB: Syntheses, structures and photoluminescent properties, *Inorg.Chim.Acta.* 360(2007)3019-3025.
- [2] V. Balzani, A. Credi, M. Venturi, *Molecular Devices and Machines*, Wiley-VCH, Weinheim, 2003.
- [3] M. Petty, *Molecular Electronics: From Principles to Practice*, Wiley, Chichester, 2008.
- [4] (a) D. Bose, J. Banerjee, S.H. Rahaman, G. Mostafa, H.-K. Fun, R. D. B. Walsh, M.J. Zaworotko, B.K. Ghosh, Polymeric end-to-end bridged cadmium(II)thiocyanates containing monodentate and bidentate N-donor organic blockers: supramolecular synthons based on π - π and/or C-H \cdots π interactions, *Polyhedron* 23 (2004) 2045-2053.
- (b) <http://dx.org/10.1039/C6RA23938B>

- (c) M. D. Kishore, D. Kumar, A review of Cadmium and Tin complexes of Schiff-base ligands, *J. Coord. Chem.* 64(2011)2130-2156.
- (d) M. Montazerzohori, M. N. -Esfahani, M. Hoseinpour, A. Naghiha, S. Zahedi, Synthesis of some new antibacterial active cadmium and mercury complexes of 4-(3-(2-(4-(dimethyl aminophenylallylidene aminopropyl-imino)prop-1-ethyl)-*N,N*-dimethyl benzene amine, *Chemical Speciation and Bioavailability* 26(2014)240-248.
- (e) <http://dx.org/10.1038/s41598-018-26483-5>
- (f) <http://dx.org/10.1016/j.micpath.2016.09.010>
- [5] (a) J. Kim Eddaoudi, N. Rosi, D. Vodak, J. Wachter, M. O'Keeffe, O.M. Yagi, Systematic Design of Pore Size and Functionality in Isoreticular MOFs and Their Application in Methane Storage, *Science* 295 (2002) 469-472.
- (b) S. Kitagawa, R. Kitaura, S.-I. Noro, Functional Porous Coordination Polymers, *Angew. Chem. Int. Ed.* 43 (2004) 2334-2375.
- [6] J. Ribas, A. Escuer, M. Monfort, R. Vicente, R. Cortes, L. Lezama, T. Rojo, Polynuclear Ni^{II} and Mn^{II} azido bridging complexes. Structural trends and magnetic behavior, *Coord. Chem. Rev.* 193 (1999) 1027-1068.
- [7] L. Mandal, S. Mandal, S. Mohanta, Syntheses, crystal structures, magnetochemistry and catechol oxidase activity of a tetracopper(II) compound and a new type of dicopper(II)-based 1D coordination polymer, *New J. Chem.* 41 (2017) 4689-4701.
- [8] S. Majumder, S. Sarkar, S. Sasmal, E.C. Sanudo, S. Mohanta, Heterobridged Dinuclear, Tetranuclear, Dinuclear-Based 1-D, and Heptanuclear-Based 1-D Complexes of Copper(II)

Derived from a Dinucleating Ligand: Syntheses, Structures, Magnetochemistry, Spectroscopy, and Catecholase Activity, *Inorg. Chem.* 50 (2011) 7540-7554.

[9] S. Sasmal, S. Sarkar, N. Aliaga-Alcalde, S. Mohanta, Syntheses, Structures, and Magnetic Properties of Three One-Dimensional End-to-End Azide/Cyanate-Bridged Copper(II) Compounds Exhibiting Ferromagnetic Interaction: New Type of Solid State Isomerism, *Inorg.Chem.* 50 (2011) 5687-5695.

[10] S. Sasmal, P. Chakraborty, S. Bhattachary N. Aliaga-Alcalde, S. Mohanta, Crystal structure and magnetic properties of a hexacopper(II)-based azide-bridged one-dimensional coordination polymer: A new pattern of azide-bridged network, *Polyhedron* 73 (2014) 67-71.

[11] Y. Ma, X.-B. Li, X.-C. Yi, Q.-X. Jia, E.-Q. Gao, C.-M. Liu, Novel Three-Dimensional Metal-Azide Network Induced by a Bipyridine-Based Zwitterionic Monocarboxylate Ligand: Structures and Magnetism, *Inorg.Chem.* 49 (2010) 8092-8098.

[12] E.-Q. Gao, P.-P. Liu, Y.-Q. Wang, Q. Yue, Q.-L. Wang, Complex Long-Range Magnetic Ordering Behaviors in Anisotropic Cobalt(II)-Azide Multilayer Systems, *Chem.- Eur. J.* 15 (2009) 1217-1226.

[13] J. -P. Zhao, Bo. -W. Hu, E.C. Sanudo, Q.Yian, Y.-F. Zeng, X.-H. Bu, Tuning the Structure and Magnetism of Azido-Mediated Cu^{II} Systems by coligand modifications, *Inorg.Chem.* 48 (2009) 2482-2489

[14] Z.-G. Gu, Y. Song, J.-L. Zuc, X.-Z. You, Chiral Molecular Ferromagnets Based on Copper(II) Polymers with End-On Azido Bridges, *Inorg. Chem.* 46 (2007) 9522-9524.

- [15] X. Liu, F. Li, X. Ma, P. CEN, S. Luo, Q. Shi, S. Ma, Y. Wu, C. Zhang, Z. Xu, W. Song, G. Xie, S. Chen, Coligand modifications fine-tuned the structure and magnetic properties of two triple-bridged azido-Cu(II) chain compounds exhibiting ferromagnetic ordering and slow relaxation, *Dalton Trans.* 46 (2017)1207-1217.
- [16] N.D. la Pinta, Z. Serna, G. Madariaga, M.K. Urriaga, M.L. Fidalgo, Robert Cortes, Ferromagnetic Interactions in an Unusual 2D Coordination Polymer Including Di-2-pyridylketone-Methoxilated Anion, (1,1)-Azide, and Rare (1,1,3,3)-Azide Bridging Ligands, *Cryst. Growth Des.* 11 (2011)1458-1461.
- [17] F.A. Fautner, F.R. Louka, J. Hofer, M. Spell, A. Lefevre, A.E. Guilbeau, Salah S. Massoud, One-Dimensional Cadmium Polymers with Alternative di(EO/EE) and di(EO/EO/EO/EE) Bridged Azide Bonding Modes, *Cryst. Growth Des.* 13 (2013) 4518-4525.
- [18] J.H. Song, K.S. Lim, D.W. Ryu, S.W. Yoon, B.J. Suh, C.S. Hong, Synthesis, Structures, and Magnetic Properties of End-to-End Azide-Bridged Manganese(III) Chains: Elucidation of Direct Magnetostructural Correlation, *Inorg.Chem.* 53 (2014)7936-7940.
- [19] O. Sengupta, P.S. Mukherjee, Mixed Azide and 5-(Pyrimidyl)tetrazole Bridged Co(II)/Mn(II) Polymers: Synthesis, Crystal Structures, Ferroelectric and Magnetic Behavior, *Inorg.Chem.* 49 (2010) 8583-8590.
- [20] S. Mukherjee, P.S. Mukherjee, Cu^{II}-azide polynuclear complexes of Cu₄ building clusters with Schiff-base co-ligands: synthesis, structures, magnetic behavior and DFT studies, *Dalton Trans.* 42 (2013) 4019-4030.

- [21] P. Roy, K. Dhara, M. Manassero, P. Banerjee, Di-, Tetra-, and Polynuclear Copper(II) Complexes: Active Catalysts for Oxidation of Toluene and Benzene, *Eur. J. Inorg. Chem.* 28 (2008) 4404-4412.
- [22] T.C. Stamatatos, K.A. Abboud, W. Wernsdorfer, G. Christou, High-Nuclearity, High-Symmetry, High-Spin Molecules: A Mixed-Valence Mn_{10} Cage Possessing Rare T symmetry and an $S=22$ Ground State*, *Angew. Chem. Int. Ed.* 45 (2006) 4134-4137.
- [23] F. Meyer, S. Demeshko, G. Leibelng, B. Kersting, E. Kaifer, H. Pritzkow, Structures and Magnetic Properties of Tetranuclear Nickel(II) Complexes with Unusual μ_3 -1,1,3 Azido Bridges, *Chem.-Eur. J.* 11 (2005) 1518-1526.
- [24] G.S. Papaefstathiou, S.P. Perleps, A. Escuer, R. Vicente, M. Font-Bardia, X. Solans, Unique Single-Atom Binding of Pseudohalogeno Ligands to Four Metal Ions Induced by Their Trapping into High-Nuclearity Cages This work was supported by CICYT (Grant BP96/0163) and the Research Committee of the University of Patras (C. Caratheodory Programme, No 1941), *Angew. Chem. Int. Ed.* 40 (2001) 884-886.
- [25] F. Meyer, P. Kircher, H. Pritzkow, Tetranuclear nickel(II) complexes with genuine μ_3 -1,1,3 and μ_4 -1,1,3,3 azide bridges, *Chem. Commun.* (2003) 774-775.
- [26] S. Sasmal, S. Hazra, P. Kundu, S. Dutta, G. Rajaraman, E.C. Sanudo, S. Mohanta, Magnetic Exchange Interactions and Magneto-Structural Correlations in Heterobridged μ -Phenoxo- $\mu_{1,1}$ -Azide Dinickel(II) Compounds: A Combined Experimental and Theoretical Exploration, *Inorg.Chem.* 50(2011)7257-7267.

- [27] S. Sasmal, S. Hazra, P. Kundu, S. Majumder, N. Aliaga-Alcalde, E. Ruiz, S. Mohanta, Magneto-Structural Correlation Studies and Theoretical Calculations of a Unique Family of Single End-to-End Azide-Bridged Ni^{II}₄ Cyclic Clusters, *Inorg.Chem.* 49 (2010) 9517-9526.
- [28] S. S. Massoud, F. R. Louka, Y.K. Obaid, R. Vicente, J. Ribas, R.C. Fischer, F.A. Mautner, Metal ions directing the geometry and nuclearity of azido-metal(II) complexes derived from bis(2-(3,5-dimethyl-1*H*-pyrazol-1-yl)ethyl)amine, *Dalton Trans.* 42 (2013) 3968-3978.
- [29] C. Adhikary, S. Koner, Structural and magnetic studies on copper (II) azido complexes, *Coord. Chem. Rev.* 254 (2010) 2933-2958.
- [30] (a) O. Ed. Khan, *Molecular Magnetism*, VCH Publishers Inc. New York, 1993.
- (b) T.W. Lane, F.M.M. Morel, A biological function for cadmium in marine diatoms, *Proc. Natl. Acad. Sci.* 97(9) (2000) 4627-4631.
- [31] A.K. Mandal, M. Suresh, P. Das, E. Suresh, M. Baidya, S.K. Ghosh, A. Das, Recognition of Hg²⁺ Ion through Restricted Imine Isomerization: Crystallographic Evidence and Imaging in Live Cells, *Org. Lett.* 14 (2012) 2980-2983.
- [32] I. Ravikumar, P. Ghosh, Zinc(II) and PPI Selective Fluorescence OFF-ON-OFF Functionality of a Chemosensor in Physiological Conditions, *Inorg.Chem.* 50 (2011) 4229-4231.
- [33] X. Liu, N. Zhang, J. Zhou, T. Chang, C. Fang, D. Shangguan, A turn-on fluorescent sensor for zinc and cadmium ions based on perylene tetracarboxylic diimide, *Analyst* 138 (2013) 901-906.

- [34] Y. W Choi, G. J. Park, Y.J. Na, H.Y. Jo, S.A. Lee, G.R.You, C. Kim, A single schiff base molecule for recognizing multiple metal ions: A fluorescence sensor for Zn(II) and Al(III) and colorimetric sensor for Fe(II) and Fe(III), *Sens. Actuators B*. 194 (2014) 343-352.
- [35] K.B. Kim, H. Kim, E.J. Song, S. Kim, I. Noh, C. Kim, A cap-type Schiff base acting as a fluorescence sensor for zinc(II) and a colorimetric sensor for iron(II), copper(II), and zinc(II) in aqueous media, *Dalton Trans.* 42 (2013) 16569-16577.
- [36] Q. He, E.W. Miller, A.P. Wong, C.J. Chang, A Selective Fluorescent Sensor for Detecting Lead in Living Cells, *J. Am. Chem. Soc.* 128 (2006) 9316-9317.
- [37] S.S. Bozkurt, S. Ayata, I. Kaynak, Fluorescence-based sensor for Pb(II) using tetra-(3-bromo-4-hydroxyphenyl)porphyrin in liquid and immobilized medium, *Spectrochim. Acta Part A*. 72 (2009) 880-883.
- [38] M. Taki, M. Desaki, A. Ojida, S. Iyoshi, T. Hirayama, I. Hamachi, Y. Yamamoto, Fluorescence Imaging of Intracellular Cadmium Using a Dual-Excitation Ratiometric Chemosensor, *J. Am. Chem. Soc.* 130 (2008) 12564-12565.
- [39] D. Ray, P.K. Bharadwaj, A Coumarin-Derived Fluorescence Probe Selective for Magnesium, *Inorg.Chem.* 47 (2008) 2252-2254.
- [40] M. Suresh, A.K. Mandal, S. Saha, E. Suresh, A. Mandoli, R.D. Liddo, P.P. Parnigotto, A. Das, Azine-Based Receptor for Recognition of Hg²⁺ Ion: Crystallographic Evidence and Imaging Application in Live Cells, *Org. Lett.* 12 (2010) 5406-5409.

- [41] L. Mandal, S. Majumder, S. Mohanta, Syntheses, crystal structures and steady state and time-resolved fluorescence properties of a PET based macrocycle and its dinuclear $Zn^{II}/Cd^{II}/Hg^{II}$ complexes, Dalton Trans. 45 (2016) 17365-17389.
- [42] L. Mandal, S. Majumder, S. Mohanta, Syntheses, Structures, and Steady State and Time Resolved Photophysical Properties of a Tetraaminodiphenol Macrocylic Ligand and Its Dinuclear Zinc(II)/Cadmium(II) Complexes with Coordinating and Noncoordinating Anions, Inorg.Chem. 51 (2012) 8739-8749.
- [43] D. J. Majumdar, S. Das, J. K. Biswas, M. Mondal, Synthesis, structure, fluorescent property, and antibacterial activity of new Cd(II) metal complex based on multidentate Schiff base ligand *N,N'*-Bis(3-methoxysalicylideneimino)-1,3-diaminopropane, J. Mol. Struct. 1134 (2017) 617-624.
- [44] D.J.Majumdar, M. S. Surendra Babu, S. Das, J.K. Biswas, M. Mondal, Synthesis, X-ray crystal structure, photo luminescent property, antimicrobial activities and DFT computational study of Zn(II) coordination polymer derived from multisite N,O donor Schiff base ligand (H_2L^1), J. Mol. Struct. 1138 (2017) 161-171.
- [45] D.J.Majumdar, M. S. Surendra Babu, S. Das, C. Mohapatra, J.K. Biswas, M. Mondal, Syntheses, X-ray Crystal Structures, Photoluminescence Properties, Antimicrobial Activities and Hirshfeld Surface of Two New Cd(II) Azide/Thiocyanate Linked Coordination Polymers, Chemistry Select 2 (2017) 4811-4822.
- [46] D.J. Majumdar, J. K. Biswas, M. Mondal, M. S. Surendra Babu, R. K. Metre, S. Das, K. Bankura, D. Mishra, Coordination of N,O-donor appended Schiff base ligand (H_2L^1) towards

Zinc(II) in presence of pseudohalides: Syntheses, crystal structures, photoluminescence, antimicrobial activities and Hirshfeld surfaces, *J. Mol. Struct.* 1155 (2018) 745-757.

[47] D.J. Majumdar, J. K. Biswas, M. Mondal, M. S. Surendra Babu, S. Das, R. K. Metre, S. S. SreeKumar, K. Bankura, D. Mishra, Cd(II) Pseudohalide Complexes with N, N'-Bis(3-ethoxysalicylideneimino) 1,3-Diaminopropane: Crystal Structures, Hirshfeld Surface, Antibacterial and Anti-Biofilm Properties, *Chemistry Select.* 3 (2018) 2912-2925.

[48] B.Valeur, *Molecular Fluorescence, Principles and Applications*, fifth ed. Wiley-VCH, Weinheim, 161 (2009).

[49] G. M. Sheldrick, *SADABS, a software for empirical absorption correction*, Ver. 2.05; University of Göttingen: Göttingen, Germany, 2002.

[50] SMART & SAINT Software Reference manuals, Version 6.45; Bruker Analytical X-ray Systems, Inc.: Madison, WI, 2003.

[51] SHELXTL Reference Manual, Ver. 6.1; Bruker Analytical X-ray Systems, Inc.: Madison, WI, 2000.

[52] G.M. Sheldrick, *SHELXTL, a software for empirical absorption correction* Ver. 6.12; Bruker AXS Inc.: WI.Madison, 2001.

[53] O. V. Dolomanov, L. J. Bourhis, R. J. Gildea, J. A. K. Howard, H. Puschmann, *OLEX2: J. Appl. Crystallogr.* 42(2009)339.

[54] K. Brandenburg, *Diamond, Ver. 3.1eM*; Crystal Impact GbR: Bonn, Germany, 2005.

[55] (a) F. Neese, The ORCA program system, *Wires Comput. Mol. Sci.* 2 (2012) 73-78. (b) F. Neese, Orca. An ab Initio Density Functional and Semiempirical Program Package version, 2009.

[56] (a) A. D. Becke, A new mixing of Hartree–Fock and local density-functional theories, *J. Chem. Phys.* 98 (1993) 1372.

(b) C. Lee, W. Yang, Development of the Colle-Salvetti correlation-energy formula into a functional of the electron density, *Phys. Rev. B.* 37 (1988) 785-789.

[57] (a) A. Schaefer, H. Horn, R. Ahlrichs, Fully optimized contracted Gaussian basis sets for atoms Li to Kr, *J. Chem. Phys.* 97 (1992) 2571-2577.

(b) F. Weigend, R. Ahlrichs, Balanced basis sets of split valence, triple zeta valence and quadruple zeta valence quality for H to Rn: Design and assessment of accuracy, *Phys. Chem. Chem. Phys.* 7 (2005) 3297-3305.

[58] M. D. Hanwell, D. E. Curtis, D. C. Lonie, T. Vandermeersch, E. Zurek, G. R. Hutchison, Avogadro: an advanced semantic chemical editor, visualization, and analysis platform, *J. Cheminform.* 4 (2012) 1758-2946-4-17.

[59] (a) T. Lu and F. Chen, Multiwfn: a multifunctional wavefunction analyzer, *J. Comp. Chem.* 33 (2012) 580-592.

(b) T. Lu, F. Chen, Calculation of Molecular Orbital Composition, *Acta Chim. Sinica.* 69 (2011) 2393-2406.

[60] (a) S.S. Sreejith, N. Mohan, M.R. P. Kurup, Experimental and theoretical studies on photoluminescent Zn(II) host complex with an open book structure: Implication on potential bioactivity and comparison with its ligand and Zn(II), Pd(II) siblings, *Polyhedron* 135 (2017) 278-295.

(b) M.J. Frisch, G.W. Trucks, H.B. Schlegel, G.E. Scuseria, M.A. Robb, J.R. Cheeseman, G. Scalmani, V. Barone, B. Mennucci, G.A. Petersson, H. Nakatsuji, M. Caricato, X. Li, H.P. Hratchian, A.F. Izmaylov, J. Bloino, G. Zheng, J.L. Sonnenberg, M. Hada, M. Ehara, K. Toyota,

R. Fukuda, J. Hasegawa, M. Ishida, T. Nakajima, Y. Honda, O. Kitao, H. Nakai, T. Vreven, Jr. J.A. Montgomery, J.e. Peralta, F. Ogliaro, M. Bearpark, J.J. Heyd, E. Brothers, K.N. Kudin, V.N. Staroverov, R. Kobayashi, J. Normand, K. Raghavachari, A. Rendell, J.C. Burant, S.S. Iyengar, J. Tomasi, M. Cossi, N. Rega, J.M. Millam, M. Klene, J.E. Knox, J.B. Cross, V. Bakken, C. Adamo, J. Jaramillo, R. Gomperts, R.E. Stratmann, O. Yazyev, A.J. Austin, R. Cammi, C. Pomelli, J.W. Ochterski, R.L. Martin, K. Morokuma, V.G. Zakrzewski, A. G. Voth, P. Salvador, J.J. Dannenberg, S. Dapprich, A.D. Daniels, ö. Farkas, J.B. Foresman, J.V. Ortiz, J. Cioslowski, D.J. Fox, *Gaussian 09*, revision A.1; Gaussian, Inc.: Wallingford, CT, 2009.

(c) E. Cancès, B. Mennucci, J. Tomasi, A new integral equation formalism for the polarizable continuum model: Theoretical background and applications to isotropic and anisotropic dielectrics, *J. Chem. Phys.* 107(1997) 3032-3041.

[61] P.A. Wayne, Clinical and Laboratory Standards Institute (CLSI)(2012).Methods for Dilution Antimicrobial Susceptibility Tests for Bacteria That Grow Aerobically; Approved Standard - Ninth Edition. 2012, 32.

[62] D. Parai, E. Islam, J. Mitra, S.K. Mukherjee, Effect of Bacoside A on growth and biofilm formation by *Staphylococcus aureus* and *Pseudomonas aeruginosa*, *Canadian Journal of Microbiology*. 63 (2017) 169-178.

[63] D.J.Majumdar, M. S. Surendra Babu, S. Das, C. Mohapatra, J.K. Biswas, M. Mondal, Syntheses, X-ray Crystal Structures, Photoluminescence Properties, Antimicrobial Activities and Hirshfeld Surface of Two New Cd(II) Azide/Thiocyanate Linked Coordination Polymers, *Chemistry Select.* 2 (2017) 4811-4822.

- [64] S. Stepanovic', D. Vukovic', V. Hola, G. Di Bonaventura, S. Djukic', I. C'irkovic', F. Ruzicka, Quantification of biofilm in microtiter plates: overview of testing conditions and practical recommendations for assessment of biofilm production by staphylococci. *J. Microbiol. Methods* 115(8) (2008) 891-899.
- [65] M. Müsken, S. Di Fiore, U. Römling, S. Häussler, A 96-well-plate-based optical method for the quantitative and qualitative evaluation of *Pseudomonas aeruginosa* biofilm formation and its application to susceptibility testing, *S.Nat. Protoc.* 5 (2010) 1460-1469.
- [66] J. Saising, L. Dube, A.-K. Ziebandt, S.P. Voravuthikunchai, M. Nega, F. Götz, Activity of Gallidermin on *Staphylococcus aureus* and *Staphylococcus epidermidis* Biofilms, *F.Agents Chemother.* 56 (2012) 5804-5810.
- [67] C.Z. Chen, S. L. Cooper, Interactions between dendrimer biocides and bacterial membranes, *Biomaterials.* 23 (2002) 3359-3368.
- [68] (a) D.J.Majumdar, M. S. Surendra Babu, S. Das, C. Mohapatra, J.K. Biswas, M. Mondal, Syntheses, X-ray Crystal Structures, Photoluminescence Properties, Antimicrobial Activities and Hirshfeld Surface of Two New Cd(II) Azide/Thiocyanate Linked Coordination Polymers, *Chemistry Select.* 2 (2017) 4811-4822.
- (b) D.J. Majumdar, J. K. Biswas, M. Mondal, M. S. Surendra Babu, S. Das, R. K. Metre, S. S. SreeKumar, K. Bankura, D. Mishra, Cd(II) Pseudohalide Complexes with N, N'-Bis(3-ethoxysalicylideneimino) 1,3-Diaminopropane: Crystal Structures, Hirshfeld Surface, Antibacterial and Anti-Biofilm Properties, *Chemistry Select.* 3 (2018) 2912-2925.

- (c) M.A.S. Goher, F.A. Mautner, K. Gatterer, M.A.M. Abu-Yussef, A.M.A. Badr, B. Sodin, C. Gspan, Four $[\text{Cd}(\text{L})_2(\text{N}_3)_2]_n$ 1D systems with different azide bridging sequences: Synthesis, spectral and structural characterization, *J. Mol. Struct.* 876 (2008) 199-205.
- (d) S. Basak, S. Sen, C. Marschner, J. Baumgartner, S. R. Batten, D. R. Turner, S. Mitra, Synthesis, crystal structures and fluorescence properties of two new di- and polynuclear Cd(II) complexes with N_2O donor set of a tridentate Schiff base ligand, *Polyhedron* 27 (2008) 1193-1200.
- (e) S. Roy, P.K. Bhaumik, K. Harms, S. Chattopadhyay, Variation in molecular and crystalline architectures of di- and poly-nuclear cadmium(II) complexes on changing the denticity of the blocking ligands, *Polyhedron* 75 (2014) 57-63.
- (f) S. Ray, S. Konar, A. Jana, S. Jana, A. Patra, S. Chatterjee, J.A. Golen, A. L. Rheingold, S.S. Mandal, S.K. Kar, Three new pseudohalide bridged dinuclear Zn(II), Cd(II) complexes of pyrimidine derived Schiff base ligands: Synthesis, crystal structures and fluorescence studies, *Polyhedron* 33 (2012) 82-89.
- (g) H. -F. Qian, Y. Dai, J. Geng, L. Wang, C. Wang, A flexible multidentate Schiff-base ligand having multifarious coordination modes in its copper(II) and cadmium(II) complexes, *Polyhedron* 67 (2014) 314-320.
- (h) F.A. Mautner, F. R. Louka, J. Hofer, M. Spell, A. Lefevre, A. E. Guilbeau, S.S. Massoud, One-Dimensional Cadmium Polymers with Alternative di(EO/EE) and di(EO/EO/EO/EE) Bridged Azide Bonding Modes, *Cryst. Growth Des.* 13 (2013) 4518-4525.

(i) S. Roy, S. Bhattacharya, S. Mohanta, Syntheses, Crystal Structures and Photophysical Aspects of Discrete and Polymeric Azido-Bridged Zinc(II) and Cadmium(II) Complexes: Sensing Properties and Structural Resemblance, *Chemistry Select.* 2 (2017) 11091-11099.

[69] W. K. Dong, Y. X. Sun, C. Y. Zhao, X. Y. Dong, L. Xu, Synthesis, structure and properties of supramolecular Mn^{II} , Co^{II} , Ni^{II} and Zn^{II} complexes containing Salen-type bisoxime ligands, *Polyhedron* 29 (2010) 2087-2097.

[70] A. B. P. Lever, *Inorganic Spectroscopy*, second ed., Elsevier, New York, 1984.

[71] J. Garcia. Sole, L.E. Bausa, D. Jaque, *An Introduction to the Optical Spectroscopy of Inorganic Solids*, John Wiley & Sons, New York, 2005.

[72] (a) A.K. Boudalis, V. Tangoulis, C.P. Raptopoulou, A. Terzis, J.P. Tuchagues, S.P. Perlepes, A new example of a tetranuclear iron(III) cluster containing the $[Fe_4O_2]^{8+}$ core: preparation, X-ray crystal structure, magnetochemistry and Moessbauer study of $[Fe_4O_2(O_2CMe)_6(N_3)_2(phen)_2]$, *Inorg. Chim. Acta.* 357 (2004) 1345-1354.

(b) M.W. Wemple, D.K. Coggin, J.B. Vincent, J.K. McCusker, W.E. Streib, J.C. Huffman, D.N. Hendrickson, G. Christou, New tetranuclear metal carboxylate clusters with the $[M_4(\mu_3-O)_2]^{8+}$ ($M = Mn^{III}$ or Fe^{III}) cores: crystal structures and properties of $[Mn_4O_2Cl_2(O_2CC_6H_3F_2-3,5)_6(py)_4]$, $[Fe_4O_2Cl_2(O_2CMe)_6(bpy)_2]$ and $[NBu^{\eta}_4][Fe_4O_2(O_2CMe)_7(pic)_2]$, *J. Chem. Soc.; Dalton Trans.* (1998) 719-726.

[73] D.J. Majumdar, J. K. Biswas, M. Mondal, M. S. Surendra Babu, S. Das, R. K. Metre, S. S. SreeKumar, K. Bankura, D. Mishra, Cd(II) Pseudohalide Complexes with N,

N'-Bis(3-ethoxysalicylideneimino) 1,3-Diaminopropane: Crystal Structures, Hirshfeld Surface, Antibacterial and Anti-Biofilm Properties, *Chemistry Select.* 3 (2018) 2912-2925.

[74] (a) F.A. Mautner, F. R. Louka, J. Hofer, M. Spell, A. Lefevre, A. E. Guilbeau, S.S. Massoud, One-Dimensional Cadmium Polymers with Alternative di(EO/EE) and di(EO/EO/EO/EE) Bridged Azide Bonding Modes, *Cryst. Growth Des.* 13 (2013) 4518-4525.

(b) F.A. Mautner, C. Berger, R.C. Fischer, S.S. Massoud, Coordination polymers of azido and thiocyanato Cd(II) and Zn(II) complexes based on 2,6-lutidine-*N*-oxide. Synthesis, characterization and luminescent properties, *Inorg. Chim. Acta.* 448 (2016) 34-41.

(c) S. Roy, P.K. Bhaumik, K. Harms, S. Chattopadhyay, Variation in molecular and crystalline architectures of di- and poly-nuclear cadmium(II) complexes on changing the denticity of the blocking ligands, *Polyhedron* 75 (2014) 57-63.

(d) H.-F. Qian, Y. Dai, J. Geng, L. Wang, C. Wang, W. Huang, A flexible multidentate Schiff-base ligand having multifarious coordination modes in its copper(II) and cadmium(II) complexes, *Polyhedron* 67 (2014) 314-320.

(e) D.J. Majumdar, M. S. Surendra Babu, S. Das, C. Mohapatra, J.K. Biswas, M. Mondal, Syntheses, X-ray Crystal Structures, Photoluminescence Properties, Antimicrobial Activities and Hirshfeld Surface of Two New Cd(II) Azide/Thiocyanate Linked Coordination Polymers, *Chemistry Select.* 2 (2017) 4811-4822.

(f) S. Roy, S. Bhattacharya, S. Mohanta, Syntheses, Crystal Structures and Photophysical Aspects of Discrete and Polymeric Azido-Bridged Zinc(II) and Cadmium(II) Complexes: Sensing Properties and Structural Resemblance, *Chemistry Select.* 2 (2017) 11091-11099.

- (g) M. Das, A. Biswas, B.K. Kundu, S. M. Mobin, G. Udayabhanu, S. Mukhopadhyay, Targeted synthesis of cadmium(II) Schiff base complexes towards corrosion inhibition on mild steel, *RSC Advances*. 7 (2017) 48569-48585.
- (h) S. Mandal, G. Rosair, D. Bandhyopadhyay, Synthesis, crystal structure and magnetic characterization of a new phenoxo-bridged binuclear manganese(III) Schiff base complex exhibiting single-molecule-magnet behavior, *Inorg. Chim. Acta*. 362 (2009) 2200-2204.
- (i) S. Chattopadhyay, M.S. Roy, M.G.B. Drew, A. Figuerola, C. Diaz, A. Ghosh, Facile synthesis of Cu(II) complexes of monocondensed N,N,N donor Schiff base ligands: Crystal structure, spectroscopic and magnetic properties, *Polyhedron* 25 (2006) 2241-2253.
- [75] (a) M. Hossein, E. Askari, M. Amirnasr, A. Amiri, T. Suzuki, Syntheses, spectral, electrochemical and thermal studies of mononuclear manganese(III) complexes with ligands derived from 1,2-propanediamine and 2-hydroxy-3 or 5-methoxybenzaldehyde: Self-assembled monolayer formation on nanostructure zinc oxide thin film, *Spectrochim. Acta Part A*. 79 (2011) 666-671.
- (b) S. Chattopadhyay, M.S. Roy, M.G.B. Drew, A. Figuerola, C. Diaz, A. Ghosh, Facile synthesis of Cu(II) complexes of monocondensed N,N,N donor Schiff base ligands: Crystal structure, spectroscopic and magnetic properties, *Polyhedron* 25 (2006) 2241-2253.
- (c) A.D. Khalaji, S. Triki, Synthesis and crystal structure of one-dimensional azide-bridged Mn(III) polymer $[\text{Mn}(\text{BrSal}_2\text{MePn})(\mu_{1,3}\text{-N}_3)]_n$ ($\text{BrSal}_2\text{MePn} = \text{N,N}'\text{-bis}(\text{salicylidene})\text{-1,2-propanediamine}$), *Russ. Coord. Chem.* 37 (2011) 518-522.
- (d) S. Mandal, G. Rosair, J. Ribas, D. Bandhopadhyay, Synthesis, crystal structure and magnetic characterization of a new phenoxo-bridged binuclear manganese(III) Schiff base complex exhibiting single-molecule-magnet behavior, *Inorg. Chim. Acta*. 362 (2009) 2200-2204.

- (e) <http://dx.org/10.1016/j.molstruc.2017.09.112>
- (f) S. Roy, S. Bhattacharya, S. Mohanta, Crystal Structures and Photophysical Aspects of Discrete and Polymeric Azido-Bridged Zinc(II) and Cadmium(II) Complexes: Sensing Properties and Structural Resemblance, *Chemistry Select.* 2 (2017) 11091-11099.
- (g) D. J. Majumdar, S. Das, J. K. Biswas, M. Mondal, Synthesis, structure, fluorescent property, and antibacterial activity of new Cd(II) metal complex based on multidentate Schiff base ligand N,N'-Bis(3-methoxysalicylideneimino)-1,3-diaminopropane, *J. Mol. Struct.* 1134 (2017) 617-624.
- (h) P. Ghorai, P. Brandao, A. Bauza, A. Frontera, A. Saha, Anion-reliant structural versatility of novel cadmium(II) complexes: Synthesis, crystal structures, photoluminescence properties and exploration of unusual O...S chalcogen bonding involving thiocyanate coligand, *Inorg. Chim. Acta.* 469 (2018) 189-196.
- (i) S. Shit, R. Sankolli, T.N. Guru Row, A Dinuclear Cadmium(II) Schiff Base Thiocyanato Complex: Crystal Structure and Fluorescence, *Acta. Chim. Slov.* 61(2014) 59-66.
- (j) S. Banerjee, A. Bauza, A. Frontera, A. Saha, Exploration of unconventional π -hole and C-H...H-C types of supramolecular interactions in a trinuclear Cd(II) and a heteronuclear Cd(II)-Ni(II) complex and experimental evidence for preferential site selection of the ligand by 3d and 4d metal ions, *RSC Adv.* 6 (2016) 39376-39386.
- (k) S. Sen, P. Talukdar, S.K. Dey, S. Mitra, G. ROsair, D.L. Hughes, G.P.A. Yap, G. Pillet, V. Gramlich, T. Matsushita, Ligating properties of a potentially tetradentate Schiff base [(CH₃)₂NCH₂CH₂N=CHC₆H₃(OH)(OMe)] with zinc(II), cadmium(II), cobalt(II), cobalt(III) and manganese(III) ions: synthesis and structural studies, *Dalton Trans.* (2006)1758-1767.

- (l) P. Ghorai, A. Dey, P. Brandao, J. Ortego-Castro, A. Bauza, A. Frontera, P.P. Roy, A. Saha, The development of a promising photosensitive Schottky barrier diode using a novel Cd(II) based coordination polymer, *Dalton Trans.* 46 (2017) 13531-13543.
- (m) J. Chakraborty, S. Thakurta, B. Samanta, A. Roy, G. Pilet, S.R. Batten, P. Jensen, S. Mitra, Synthesis, characterisation and crystal structures of three trinuclear cadmium(II) complexes with multidentate Schiff base ligands, *Polyhedron* 26 (2007) 5139-5149.
- (n) P. Chakraborty, S. Majumder, A. Jana, S. Mohanta, Syntheses, structures, catecholase activity, spectroscopy and electrochemistry of a series of manganese(III) complexes: Role of auxiliary anionic ligand on catecholase activity, *Inorg. Chim. Acta.* 410 (2014) 65-75.
- (o) N. Sarkar, M.G.B. Drew, K. Harms, A. Bauza, A. Frontera, S. Chattopadhyay, Methylene spacer regulated variation in conformation of tetradentate N₂O₂ donor Schiff bases trapped in manganese(III) complexes, *CrystEngComm.* 20 (2018) 1077-1086.
- (p) S. Ghosh, S. Roy, C. Liu, S. Mohanta, A nickel(ii)-manganese(ii)-azido layered coordination polymer showing a three-dimensional ferrimagnetic order at 35 K, *Dalton Trans.* 47 (2018) 836-844.
- (r) S. Mondal, P. Chakraborty, N. Aliaga-Alcalde, S. Mohanta, Syntheses, crystal structures and magnetic properties of three bis(end-on azide) bridged dicopper(II) complexes derived from half-condensed ligands: Observation of the smallest Cu–azide–Cu bridge angle in dinuclear systems, *Polyhedron* 63 (2013) 96-102.
- (s) <https://doi.org/10.1016/j.poly.2017.12.037>

(x) N. Hari, A. Jana, S. Mohanta, Syntheses, crystal structures and ESI-MS of mononuclear–dinuclear, trinuclear and dinuclear based one-dimensional copper(II)–s block metal ion complexes derived from a 3-ethoxysalicylaldehyde–diamine ligand, *Inorg. Chim. Acta.* 467 (2017) 11-20.

(y) S. Hazra, J. Titis, D. Valigura, R. Boca, S. Mohanta, Bis-phenoxido and bis-acetato bridged heteronuclear $\{\text{Co}^{\text{III}}\text{Dy}^{\text{III}}\}$ single molecule magnets with two slow relaxation branches, *Dalton Trans.* 45 (2016) 7510-7520.

(z) S. Roy, S. Bhattacharya, S. Mohanta, Crystal Structures and Photophysical Aspects of Discrete and Polymeric Azido-Bridged Zinc(II) and Cadmium(II) Complexes: Sensing Properties and Structural Resemblance, *Chemistry Select.* 2 (2017)11091-11099.

[76] S.S. Sreejith, N. Mohan, M.R. P. Kurup, Experimental and theoretical studies on photoluminescent Zn(II) host complex with an open book structure: Implication on potential bioactivity and comparison with its ligand and Zn(II), Pd(II) siblings, *Polyhedron* 135 (2017) 278-295.

[77] (a) D.J. Majumdar, J. K. Biswas, M. Mondal, M. S. Surendra Babu, S. Das, R. K. Metre, S.S. Sree Kumar, K. Bankura, D. Mishra, Cd(II) Pseudohalide Complexes with N, N'-Bis(3-ethoxysalicylideneimino) 1,3-Diaminopropane: Crystal Structures, Hirshfeld Surface, Antibacterial and Anti-Biofilm Properties, *Chemistry Select.* 3(2018) 2912-2925

(b) D.J.Majumdar, M. S. Surendra Babu, S. Das, C. Mohapatra, J.K. Biswas, M. Mondal, Syntheses, X-ray Crystal Structures, Photoluminescence Properties, Antimicrobial Activities and

Hirshfeld Surface of Two New Cd(II) Azide/Thiocyanate Linked Coordination Polymers, *Chemistry Select.* 2 (2017) 4811-4822.

(c) M. Das, A. Biswas, B.K. Kundu, S. M. Mobin, G. Udayabhanu, S. Mukhopadhyay, Targeted synthesis of cadmium(II) Schiff base complexes towards corrosion inhibition on mild steel, *RSC Advances.* 7 (2017) 48569-48585.

(d) P. Chakraborty, A. Guha, S. Das, e. Zangrando, D. Das, Phenoxo bridged luminescent dinuclear zinc(II) and cadmium(II) complexes of 2-[[[2-(2-pyridyl)ethyl]imino]methyl]phenol: Crystal structure, photophysical and thermal studies, *Polyhedron* 49 (2013) 12-18

(e) P. Kundu, E. Zangrando, P. Chakraborty, Coordinating and non-coordinating anion controlled synthesis of different nuclearity cadmium(II) complexes of 2-((E)-((pyridin-2-yl)methylimino)methyl)phenol: Crystal structure and photophysical study, *Polyhedron* 101 (2015) 6-13.

(f) D. J. Majumdar, S. Das, J. K. Biswas, M. Mondal, Synthesis, structure, fluorescent property, and antibacterial activity of new Cd(II) metal complex based on multidentate Schiff base ligand *N,N'*-Bis(3-methoxysalicylideneimino)-1,3-diaminopropane, *J. Mol. Struct.* 1134 (2017) 617-624.

(g) S. Roy, S. Bhattacharya, S. Mohanta, Syntheses, Crystal Structures and Photophysical Aspects of Discrete and Polymeric Azido-Bridged Zinc(II) and Cadmium(II) Complexes: Sensing Properties and Structural Resemblance, *Chemistry Select.* 2(2017) 11091-11099.

(h) S. Konar, An unprecedented 2D Cd(II) coordination polymer with 3,6 connected binodal net of pyrimidine derived schiff base ligand: Synthesis, crystal structure and spectral studies, *Inorg.Chem. Commun.* 49 (2014) 76-78.

(i) S. Ray, S. Konar, A. Jana, S. Jana, A. Patra, S. Chatterjee, J.A. Golen, A. L. Rheingold, S.S. Mandal, S.K. Kar, Three new pseudohalide bridged dinuclear Zn(II), Cd(II) complexes of pyrimidine derived Schiff base ligands: Synthesis, crystal structures and fluorescence studies, *Polyhedron* 33 (2012) 82-89.

(j) S. Shit, R. Sankolli, T.N. Guru Row, A Dinuclear Cadmium(II) Schiff Base Thiocyanato Complex: Crystal Structure and Fluorescence, *Acta. Chim. Slov.* 61 (2014) 59-66.

(k) F. Chen, M.-F. Wa, G.-N. Liu, M.-S. Wang, Fa.-K. Zheng, C. Yang, z.-n. Xu, Z.-Fa. Liu, G.-C. Guo, J.-S. Huang, Zinc(II) and Cadmium(II) Coordination Polymers Based on 3-(5*H*-Tetrazolyl)benzoate Ligand with Different Coordination Modes: Hydrothermal Syntheses, Crystal Structures and Ligand-Centered Luminescence, *Eur. J.Inorg. Chem.* 31 (2010) 4982-4991.

[78] J.R. Lakowicz, Topics in Fluorescence Spectroscopy, *Plenum Press, New York*, 1994.

[79] S. Ray, S. Konar, A. Jana, S. Patra, S. Chatterjee, J.A. Golen, A.L. Rheingold, S. Mandal, S.K. Kar, Three new pseudohalide bridged dinuclear Zn(II), Cd(II) complexes of pyrimidine derived Schiff base ligands: Synthesis, crystal structures and fluorescence studies, *Polyhedron* 33 (2012) 82-89.

[80] W. Gan, S.B. Jones, J.H. Reibenspies, R.D. Hancock, A fluorescent ligand rationally designed to be selective for zinc(II) over larger metal ions. The structures of the zinc(II) and

cadmium(II) complexes of *N,N*-bis(2-methylquinoline)-2-(2-aminoethyl)pyridine, *Inorg. Chim. Acta.* 358 (2005) 3958-3966.

[81] (a) Y. Li, L. Shi, L.-X. Qin, L.-L. Qu, C. Jing, M. Lan, T.D. James, Y.-T. Long, An OFF-ON fluorescent probe for Zn^{2+} based on a GFP-inspired imidazolone derivative attached to a 1,10-phenanthroline moiety, *Chem. Commun.* 47(2011)4361-4363.

(b) P. Ciesla, P. Kocot, P. Mytych, Z. Stasicka, Homogeneous photocatalysis by transition metal complexes in the environment, *J. Mol. Catal. A.Chem.* 224 (2004) 17-33.

(c) Jr. A.Valek, The life and times of excited states of organometallic and coordination compounds, *Coord. Chem. Rev.* 200(2000)(933-978).

(d) A.P. de Silva, D.P. Fox, A.J. Huxley, T.S. Moody, Combining luminescence, coordination and electron transfer for signalling purposes, *Coord. Chem. Rev.* 205 (2000) 41-57.

(e) Da-Wei Fu, Hong-Ling Cai, Yuanming Liu, Qiong Ye, Wen Zhang, Yi Zhang, Xue-Yuan Chen, Gianluca Giovannetti, Massimo Capone, Jiangyu Li, Ren-Gen Xiong, Diisopropylammonium Bromide Is a High-Temperature Molecular Ferroelectric Crystal, *Science* 339 (2013) 425-428.

(f) Da-Wei Fu, Wen Zhang, Hong-Ling Cai, Yi Zhang, Jia-Zhen Ge, Ren-Gen Xiong, Songping D. Huang, Supramolecular Bola-Like Ferroelectric: 4-Methoxyanilinium Tetrafluoroborate-18-crown-6, *J. Am. Chem. Soc.* 133 (2011) 12780-12786.

(g) Da-Wei Fu, Wen Zhang, Hong-Ling Cai, Jia-Zhen Ge, Yi Zhang, Ren-Gen Xiong, Diisopropylammonium Chloride: A Ferroelectric Organic Salt with a High Phase Transition

Temperature and Practical Utilization Level of Spontaneous Polarization, *Adv. Mater.* 23 (2011) 5658-5662.

(h) Da-Wei Fu, Hong-Ling Cai, Shen-Hui Li, Qiong Ye, Lei Zhou, Yi Zhang, Feng Deng, Ren-Gen Xiong, 4-Methoxyanilinium Perrhenate 18-Crown-6: A New Ferroelectric with Order Originating in Swinglike Motion Slowing Down, *Phys. Rev. Lett.* 110 (2013) 257601.

(i) Wan-Ying Zhang, Yuan-Yuan Tang, Peng-Fei Li, Ping-Ping Shi, Wei-Quang Liao, Da-Wei Fu, Heng-Yun Ye, Yi Zhang, Ren-Gen Xiong, Precise Molecular Design of High- T_c 3D Organic-Inorganic Perovskite Ferroelectric: [MeHdabco]RbI₃ (MeHdabco = *N*-Methyl-1,4-diazoniabicyclo[2.2.2]octane), *J. Am. Chem. Soc.* 139 (2017) 10897-10902.

[82] S. Basak, S. Sen, S. Banerjee, S. Mitra, G. Rosair, M.T.G. Rodriguez, Three new pseudohalide bridged dinuclear Zn(II) Schiff base complexes: Synthesis, crystal structures and fluorescence studies, *Polyhedron* 26 (2007) 5104-5112.

[83] D. Sadhukhan, A. Ray, G. Rosair, L. Charbonniere, S. Mitra, Cobalt(II), Manganese(IV) Mononuclear and Zinc(II) Symmetric Dinuclear Complexes of an Aliphatic Hydrazone Schiff Base Ligand with Diversity in Coordination Behaviors and Supramolecular Architectures: Syntheses, Structural Elucidations, and Spectroscopic Characterizations, *Bull. Chem. Soc. Jpn.* 84 (2011) 764-777.

[84] M. Maiti, D. Sadhukhan, S. Thakurta, S. Roy, G. Pilet, R.J. Butcher, A. Nonat, L.J. Charbonniere, S. Mitra, Series of Dicyanamide-Interlaced Assembly of Zinc-Schiff-Base Complexes: Crystal Structure and Photophysical and Thermal Studies, *Inorg. Chem.* 51 (2012) 12176-12187.

- [85] (a) D.J. Majumdar, J. K. Biswas, M. Mondal, M. S. Surendra Babu, S. Das, R. K. Metre, S. S. SreeKumar, K. Bankura, D. Mishra, Cd(II) Pseudohalide Complexes with N, N'-Bis(3-ethoxysalicylideneimino) 1,3-Diaminopropane: Crystal Structures, Hirshfeld Surface, Antibacterial and Anti-Biofilm Properties, *Chemistry Select.* 3 (2018) 2912-2925.
- (b) D. Sadhukhan, A. Ray, G. Rosair, L. Charbonniere, S. Mitra, Cobalt(II), Manganese(IV) Mononuclear and Zinc(II) Symmetric Dinuclear Complexes of an Aliphatic Hydrazone Schiff Base Ligand with Diversity in Coordination Behaviors and Supramolecular Architectures: Syntheses, Structural Elucidations, and Spectroscopic Characterizations, *Bull. Chem. Soc. Jpn.* 84 (2011) 764-777.
- (c) M. Maiti, D. Sadhukhan, S. Thakurta, S. Roy, G. Pilet, R.J. Butcher, A. Nonat, L.J. Charbonniere, S. Mitra, Series of Dicyanamide-Interlaced Assembly of Zinc-Schiff-Base Complexes: Crystal Structure and Photophysical and Thermal Studies, *Inorg. Chem.* 51 (2012) 12176-12187.
- (d) D.J. Majumdar, J. K. Biswas, M. Mondal, M. S. Surendra Babu, S. Das, R. K. Metre, S. S. SreeKumar, K. Bankura, D. Mishra, Cd(II) Pseudohalide Complexes with N, N'-Bis(3-ethoxysalicylideneimino) 1,3-Diaminopropane: Crystal Structures, Hirshfeld Surface, Antibacterial and Anti-Biofilm Properties, *Chemistry Select.* 3 (2018) 2912-2925.
- (e) D.J. Majumdar, M. S. Surendra Babu, S. Das, C. Mohapatra, J.K. Biswas, M. Mondal, Syntheses, X-ray Crystal Structures, Photoluminescence Properties, Antimicrobial Activities and Hirshfeld Surface of Two New Cd(II) Azide/Thiocyanate Linked Coordination Polymers, *Chemistry Select.* 2 (2017) 4811-4822.

- (f) I. Nawrot, B. Machura, R. Kriszynski, Coordination assemblies of Cd^{II} with 2,2':6',2''-terpyridine (terpy), 2,3,5,6-tetra-(2-pyridyl)pyrazine (tppz) and pseudohalide ions – structural diversification and luminescence properties, *Cryst. Eng.Com.* 17 (2015) 830-845.
- (g) S. Roy, S. Bhattacharya, S. Mohanta, Syntheses, Crystal Structures and Photophysical Aspects of Discrete and Polymeric Azido-Bridged Zinc(II) and Cadmium(II) Complexes: Sensing Properties and Structural Resemblance, *Chemistry Select.* 2 (2017) 11091-11099.
- (h) D.J.Majumdar, M. S. Surendra Babu, S. Das, C. Mohapatra, J.K. Biswas, M. Mondal, Syntheses, X-ray Crystal Structures, Photoluminescence Properties, Antimicrobial Activities and Hirshfeld Surface of Two New Cd(II) Azide/Thiocyanate Linked Coordination Polymers, *Chemistry Select.* 2 (2017) 4811-4822.
- (i) S. Roy, S. Chattopadhyay, Mono, di and trinuclear photo-luminescent cadmium(II) complexes with N₂O and N₂O₂ donor salicylidimine Schiff bases: Synthesis, structure and self assembly, *Inorg.Chim.Acta.* 433 (2015) 72-77.
- (j) S. Roy, K. Harms, S. Chattopadhyay, Formation of three photoluminescent dinuclear cadmium (II) complexes with Cd₂O₂ cores, *Polyhedron* 91 (2015) 10-17.
- [86] (a) D.J.Majumdar, M. S. Surendra Babu, S. Das, C. Mohapatra, J.K. Biswas, M. Mondal, Syntheses, X-ray Crystal Structures, Photoluminescence Properties, Antimicrobial Activities and Hirshfeld Surface of Two New Cd(II) Azide/Thiocyanate Linked Coordination Polymers, *Chemistry Select* 2 (2017) 4811-4822.
- (b) <https://doi.org/10.1016/j.ica.2015.10.015>

- (c) Syntheses, structures and bioactivities of cadmium(II) complexes with a tridentate heterocyclic N- and S-ligand, J.-A. Zhang, M. Pan, J. -Y. Zhang, B. -S. Kang, C. -Y. Su, *Inorg. Chim. Acta.* 362(2009)3519-25.
- (d) M. Montazerzohoria, M. Nasr-Esfahania, M. Hoseinpoura, A. Naghiha, S. Zahedia, Synthesis of some new antibacterial active cadmium and mercury complexes of 4-(3-(2-(4-(dimethyl aminophenylallylidene aminopropyl-imino)prop-1-ethyl)-*N,N*-dimethylbenzene amine, *Chemical Speciation & Bioavailability* 26(2014)240-48.
- (e) M. D. Kishore, D. Kumar, Review of Cadmium and Tin complexes of Schiff-base ligands, *J. Coord. Chem.* 64(2011)2130-2156.
- (f) <https://doi.org/10.1016/j.molstruc.2017.09.015>
- (g) <https://doi.org/10.1016/j.molstruc.2017.10.074>
- (h) <https://doi.org/10.1007/s12039-018-1438-z>
- (i) M. Gelmi, P. Apostoli, E. Cabbibo, S. Porrus, L. Alessio, A. Turano, Resistance of cadmium salts and metal absorption by different microbial species, *Current Microbiology* 29(1994)335-341.
- (j) L. Saghatforoush, L. V. Matarranz, F. Chalabian, S. Ghammamy, F. Katouzian, Synthesis of cadmium complexes of 4-chloro-terpyridine: From discrete dimer to 1D chain polymer, crystal structure and antibacterial activity, *J. Chem. Sci.* 124(2012)577-585.
- [87] (a) D.J. Majumdar, M. S. Surendra Babu, S. Das, C. Mohapatra, J.K. Biswas, M. Mondal, Syntheses, X-ray Crystal Structures, Photoluminescence Properties, Antimicrobial Activities and Hirshfeld Surface of Two New Cd(II) Azide/Thiocyanate Linked Coordination Polymers, *Chemistry Select.* 2 (2017) 4811-4822.

(b) G.C. Guo, T.C.W. Mak, A μ -1,1,1,3,3,3 Azide Anion inside a Trigonal Prism of Silver Centers, *Angew. Chem. Int. Ed. Engl.* 37 (1998) 3268-3270.

(c) D.J. Majumdar, J. K. Biswas, M. Mondal, M. S. Surendra Babu, S. Das, R. K. Metre, S. S. SreeKumar, K. Bankura, D. Mishra, Cd(II) Pseudohalide Complexes with N, N'-Bis(3-ethoxysalicylideneimino) 1,3-Diaminopropane: Crystal Structures, Hirshfeld Surface, Antibacterial and Anti-Biofilm Properties, *Chemistry Select.* 3 (2018) 2912-2925.

Table 1 Photo-physical parameters of Schiff base ligands (H_2L^{OMe}/H_2L^{OEt}) and tetranuclear Cd(II) complexes in DMSO at room temperature (298 K)

Compound	Absorption (λ_{max}), nm	Excitation (λ_{max}), nm	Emission (λ_{max}), nm
Ligand(H_2L^{OMe})	264, 332, 427	333	500
Ligand(H_2L^{OEt})	264, 333, 427	333	501
Cd ^{II} complex (1)	285, 372	372	519
Cd ^{II} complex (2)	285, 373	373	516

Table 2 Quantum yield (Φ) values comparison of salen-type ligands, tetranuclear Cd(II) complexes and other reported important cadmium(II) complexes

Compounds	Quantum yield (Φ)	References
Schiff base(HL^{OMe})	0.00353,	This work
Schiff base(HL^{OEt})	0.01308	This work
Identical Schiff base(H_2L^{OEt})	4.6×10^{-3}	a
Identical Schiff base (H_2L^{OMe})	8.9×10^{-3}	b
Identical Schiff base (H_2L^0)	9.3×10^{-3}	c
$[Cd_2L^{OMe}(\mu_{1,1}-N_3)(\mu_{1,3}-N_3)]_n$ (1)	0.02742	This work
$[Cd_4(L^{OEt})_2(\mu_{1,1}-N_3)_3(OAc)]_2$	0.02872	This work
$[Cd_4(L^{OEt})_2(\mu_{1,1}-N_3)_3(\eta^1-N_3)]_2$	0.03767	d
$[Cd_4(N_3)_4(L^1) \cdot H_2O]_n$	0.03410	e
$[Cd(N_3)(NO_3)(terpy)(H_2O)]$	<0.1	f

$[\text{Cd}_2(\mu_{1,1}\text{-N}_3)_2(\text{N}_3)_2(\text{terpy})_2]$	<0.1	f
$[\text{Cd}_3^{\text{II}}(\text{N}_3)_4(\text{L}^2)_2]_n$	0.0236	g
$[\text{Cd}_2^{\text{II}}(\text{N}_3)_3(\text{L}^1)]_n$	0.0067	
$[\text{Cd}_4(\text{SCN})_4(\text{L}^1)_2]_n$	0.0370	h
$[\text{Cd}_2(\text{L}^2)_2(\text{SCN})_2(\text{CH}_3\text{OH})]$	0.0330	i
$[\text{Cd}_2(\text{L}^3)_2(\text{NO}_3)_2]$	0.03219	j

Table 3A MIC ($\mu\text{g/mL}$) and bacterial growth inhibition zone diameter (mm) against the complexes (**1** and **2**) and the ligands ($\text{H}_2\text{L}^{\text{OMe}}/\text{H}_2\text{L}^{\text{OEt}}$) of the tested bacterial strains.

Bacteria	Complex 1=S1		Complex 2=S2		$\text{H}_2\text{L}^{\text{OMe}} = \text{L1}$		$\text{H}_2\text{L}^{\text{OEt}} = \text{L2}$	
	MIC	Growth inhibition zone (mm)	MIC	Growth inhibition zone (mm)	MIC	Growth inhibition zone (mm)	MIC	Growth inhibition zone (mm)
<i>B. subtilis</i>	58	9.89 ± 0.55	54	10.62 ± 0.91	550	4.13 ± 0.28	500	4.35 ± 0.51
<i>E. gallinarum</i>	54	11.37 ± 0.83	42	12.29 ± 0.74	500	5.89 ± 0.31	450	5.13 ± 0.62
<i>P. vulgaris</i>	46	12.81 ± 0.59	40	13.48 ± 0.62	350	7.94 ± 0.22	300	8.29 ± 0.42
<i>E. aerogenes</i>	52	10.51 ± 0.43	38	12.84 ± 0.59	450	6.67 ± 0.41	400	7.68 ± 0.19

Table 3B MIC ($\mu\text{g/mL}$) and bacterial growth inhibition zone diameter [GIC] (mm) against some important reported Cd(II) Schiff base complexes tested bacterial Strains

Bacteria	<i>B. subtilis</i>		<i>E. gallin</i>	<i>P. vulgaris</i>			<i>E. aerogenes</i>		Ref 86
	MIC	GIC (mm)	<i>m</i> MIC	GIC (mm)	MIC	GIC (mm)	MIC	GIC (mm)	
{[Cd ₄ (N ₃) ₄ (L1) ₂].(H ₂ O) _n	30	8.4	-	-	30	7.8	140	5.8	a
[Cd ₄ (SCN) ₄ (L1) ₂] _n	20	7.3	-	-	20	8.8	140	6.5	
[Cd(valp) ₂ (imidazole) ₂]	10	100%					10	60-70%	b
[Cd(valp) ₂ (phen)H ₂ O]	15	60-70%					15		
[CdL ₂](ClO ₄) ₂	-	-	>128	-	-	-	0.78	-	c
[Cd(L)Br ₂]			>128				25		
[Cd ₂ (L) ₂ (NO ₃) ₄]			>128				6.25		
[Cd ₂ (L) ₂ I ₄],			>128				1.56		
CdLCl ₂	125	28.20	-	-	-	-	-	-	d
CdLBr ₂	37	28.00							
CdLI ₂	125	25.30							
CdL(NCS) ₂	125	27.42							
[Cd(NS) ₂]	50,00 0	19					781	²⁰	e
[Cd(MP ₂ OATA)Cl ₂] ₂	40	5.5±0.3	-	-	35	3.8±0.2	175	5.5±0.3	

$[\text{CdL}^+(\text{ClO}_4)_2]\text{CH}_3\text{CN}$	4	50 ± 5	-	-	-	-	-	-	g
--	---	------------	---	---	---	---	---	---	---

Table 3B MIC ($\mu\text{g/mL}$)/GIC of some important Cadmium salts against tested bacterial Strains

Bacteria	<i>B.Cereus</i>	<i>S.aureus</i>		<i>S.typi</i>	<i>P.aeruginosa</i>		<i>E.coli</i>		<i>B.subtilis</i>	<i>C.albicans</i>	Ref
											86
$\text{Cd}(\text{ClO}_4)_2$	10	8		8	7		-		-	-	h
$\text{Cd}(\text{NO}_3)_2$	-	125		500	>1000					62.5	i
CdSO_4	-	125		500	>1000		-		-	62.5	i
CdCl_2	-	62.5		125	500		-		-	62.5	i
CdI_2	42	39		38	-		35		-	-	i
		MIC	GIC		MIC	GIC	MIC	GIC			
$\text{Cd}(\text{OAc})_2$		-	-		6.25	35	3.12	40			j

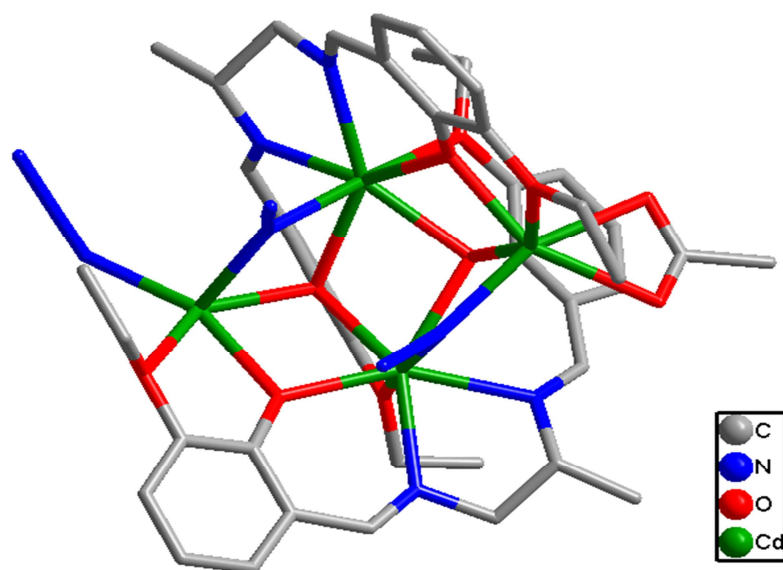


Fig.1. The perspective view of the asymmetric unit of complex 2

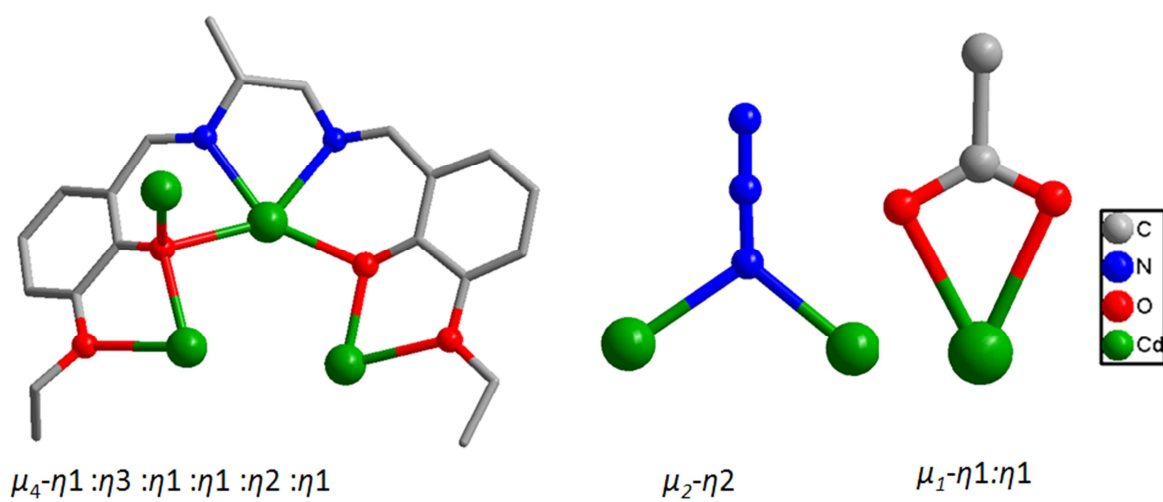


Fig.2. Bindings mode of ligand $[\text{L}^{\text{OEt}}]^{2-}$, azido and acetate anion

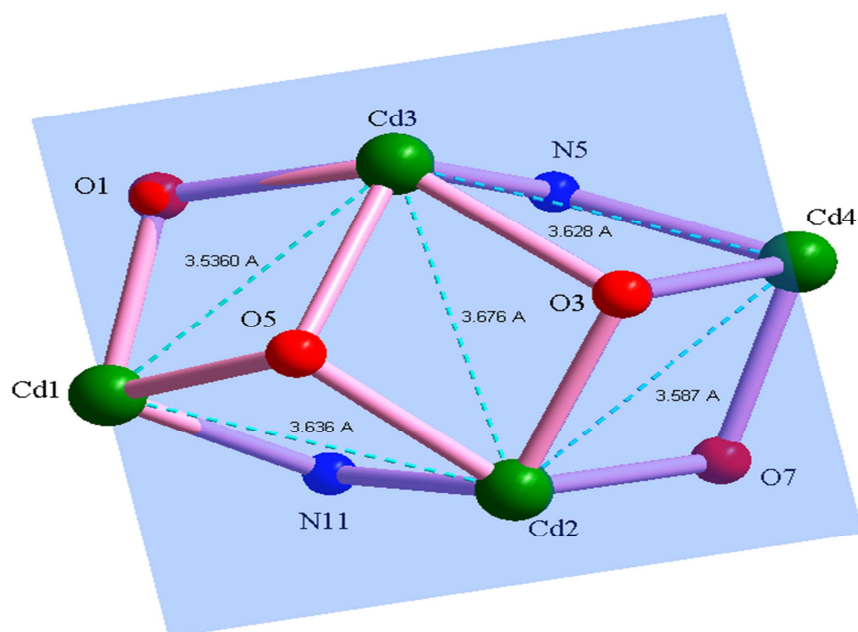


Fig.3. Butterfly shaped tetrameric core in complex 2

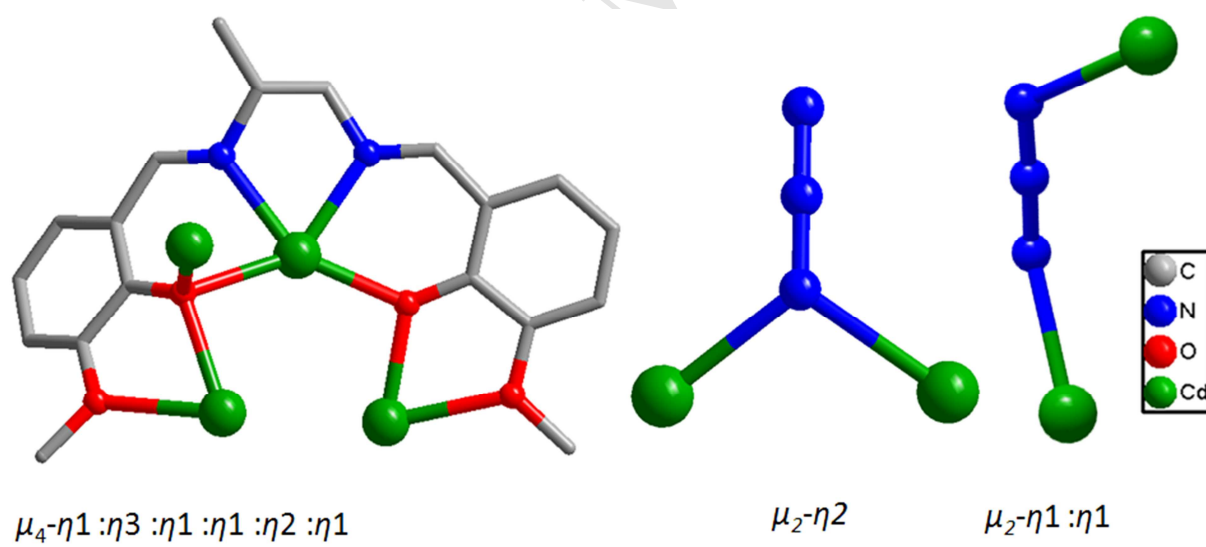


Fig.4. Bindings mode of ligand $[L_1]^{2-}$ and azide ion

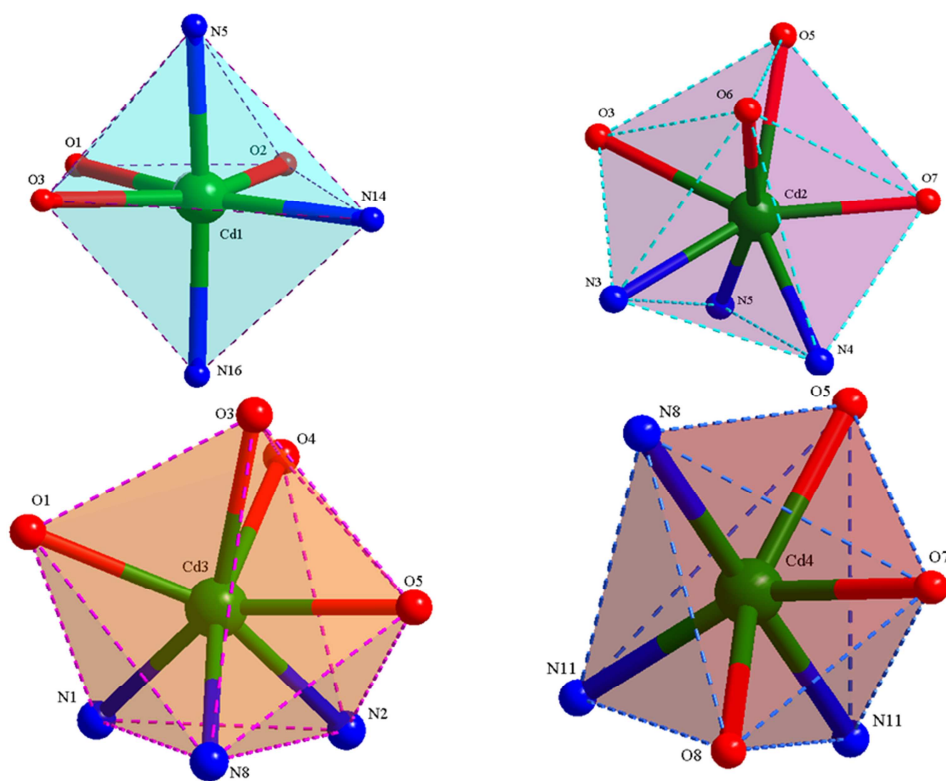


Fig.5. Metal coordination geometry in complex 1

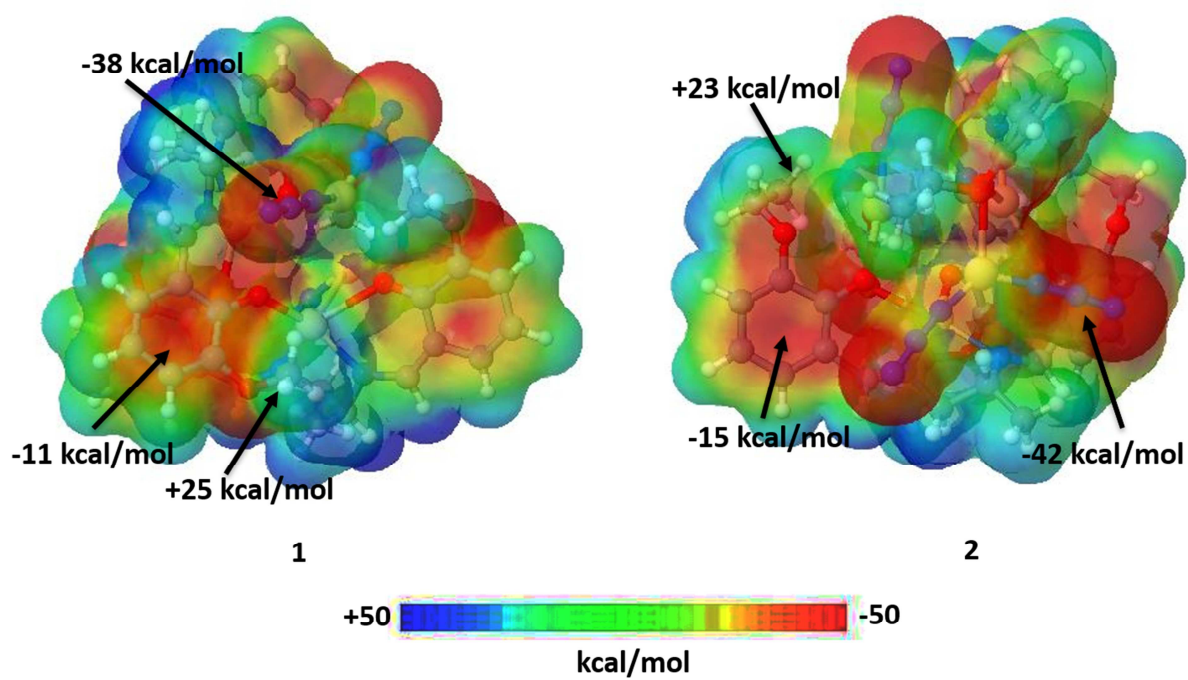


Fig.6. Electrostatic potential map of complex 1 and complex 2 on electron density isosurface computed at the B3LYP/def2-TZVP level of theory.

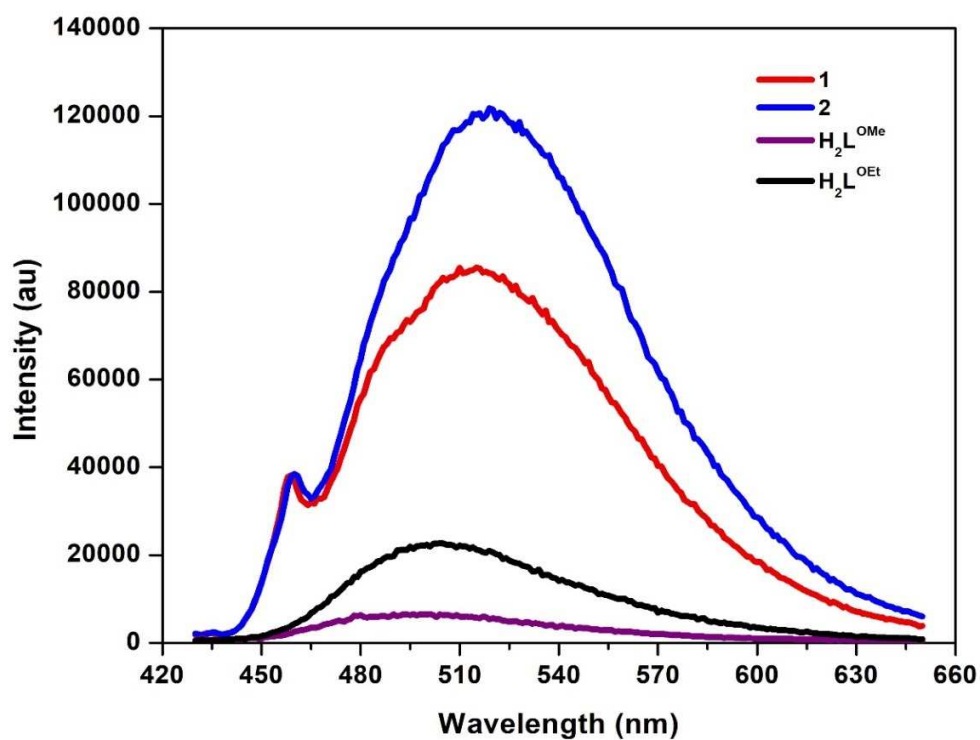


Fig. 7. Ligand centered emission spectra of ligands ($\text{H}_2\text{L}^{\text{OMe}}/\text{H}_2\text{L}^{\text{OEt}}$) and tetranuclear Cd(II) complexes in DMSO at 298K

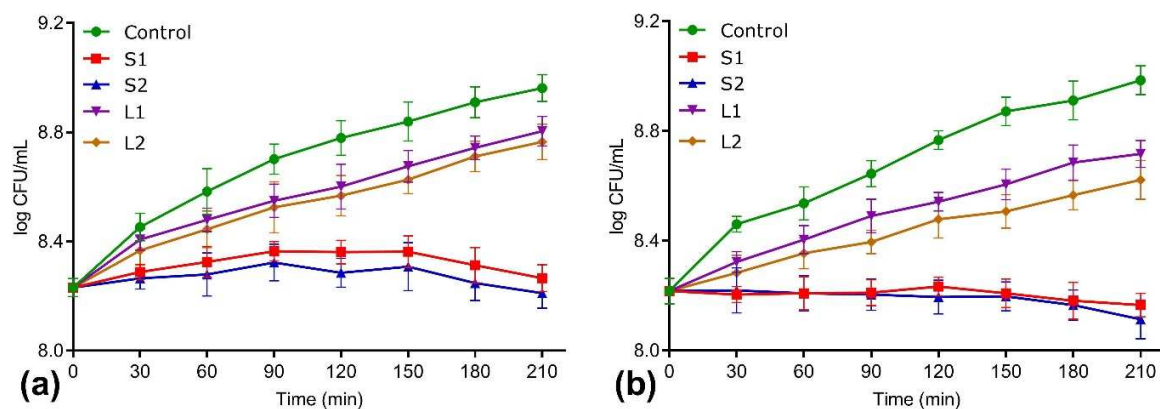


Fig.8. Time-kill curves of (a) *E. gallinarum* and (b) *P. vulgaris* against the Cd (II) complexes (**1** and **2**) and the ligands (H_2L^{OMe}/H_2L^{OEt}). All data were taken in triplicate and error bars shows standard deviation

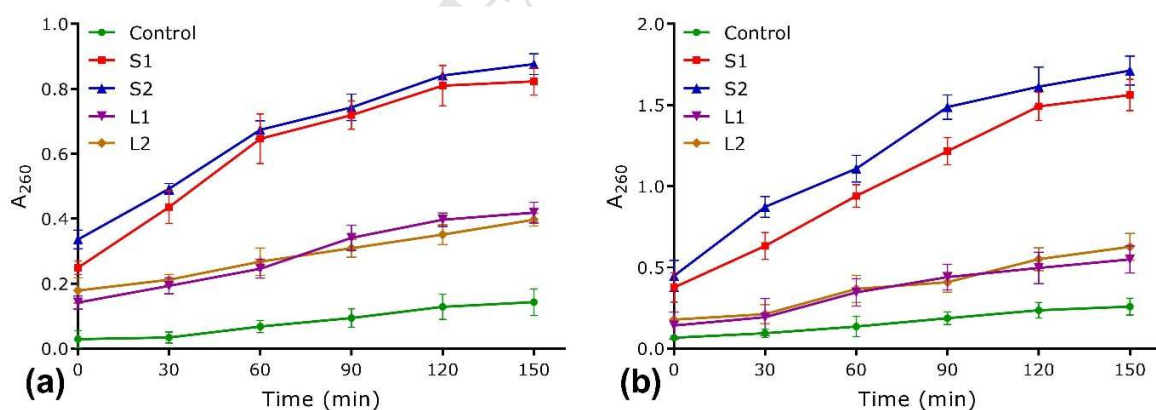


Fig.9. Membrane damage efficiency of the complexes (**1** and **2**) and the ligands (H_2L^{OMe}/H_2L^{OEt}) against (a) *E. gallinarum* and (b) *P. vulgaris*

HIGHLIGHTS

- Two Cd(II) complexes were synthesized and characterized
- Single X-ray crystallography
- DFT and TD-DFT calculations
- Photo physical properties of the complexes were investigated
- Antimicrobial and anti bio-film properties were evaluated